New Solutions for Two-Cell Vortices

FANI I. MANIKIS

A Thesis

In The Department

Of

Mechanical Engineering

Presented in Partial Fulfillment of the Requirements

for the Degree of Master of Applied Science (Mechanical Engineering)

at Concordia University

Montreal, Quebec, Canada

August 2015

© Fani I. Manikis 2015

Concordia University

School of Graduate Studies

CONCORDIA UNIVERSITY

SCHOOL OF GRADUATE STUDIES

This is to certify that the Thesis prepared,

By: **Fani Manikis**

Entitled: **"New Solutions for Two-Cell Vortices"**

and submitted in partial fulfillment of the requirements for the Degree of

Master of Applied Science (Mechanical Engineering)

complies with the regulations of this University and meets the accepted standards with respect to originality and quality.

Signed by the Final Examining Committee:

Dr. S. Rakheja	Chair
Dr. H.D. Ng	Examiner
Dr. S. Li Building, Civil and Environmental Engineering	Examiner External
Dr. G. Vatistas	Supervisor

Approved by:

Dr. S. Narayanswamy, MASc Program Director
Department of Mechanical and Industrial Engineering

Dr. Amir Asif, Dean
Faculty of Engineering & Computer Science

Date: _____

Abstract

Fani I. Manikis

Two celled incompressible vortices are known from the work of Sullivan (1959). This dissertation first extends the previously derived wider latitude, incompressible, steady two-cell vortex of Vatistas (1998) to account for the effects of time as it decays. Then, it is also broadened to simulate steady vortices where the density variation is included.

Based on the conservation of mass and momentum equations, a new method to analytically characterize two-cell decaying vortices is presented. The study shows that the core radius increases linearly with time, while the maximum velocity reduces hyperbolically. In comparison to Lamb (1932) - Oseen (1912) one-cell vortex, the dominant tangential velocity in the two-celled type is shown to decline considerably faster. Both effects are attributed to the increased viscous dissipation. Based on theoretical grounds, it is argued that the cause of the previously discovered vortex strength reduction in wing tip vortices with an externally imposed central jet is due to the switch of the one cell tip vortex into a two-cell, and not due to the added turbulence caused by the jet.

Because Sullivan's vortex assumes an unbounded radial velocity in the radial direction, its extension to compressible kind, taking into account the convective heat transfer in the energy equation, is not possible without some very drastic simplifications concerning the problem. In this dissertation an alternate approach to the problem is offered where the previous weakness is absent. The earlier contribution of Vatistas (1998) *vis-à-vis* incompressible two-cell vortices is now generalized to account for density variation. The conservation equations of mass, momentum and energy are abridged assuming intense vortex conditions. The system of equations, describing the thermal side of the problem is brought into a closure via the inclusion of the equation of state for a calorically perfect gas. The temperature, density and pressure are then calculated using straightforward, readily available, numerical integration software.

It is found that along the converging flow direction, the temperature first decreases (in the outer cell), increases within the inner cell, and then flattens close to the vortex center. The cause of this effect is identified to be due to the interplay of dilation-contraction and mechanical dissipation in the infinitesimal fluid element. Density and pressure near the axis, where the whirl is cold, are shown to be under sub ambient conditions, i.e. the gas density is thinner and the pressure is under vacuum conditions. All these properties depend strongly on the vortex Mach number.

Acknowledgments

First of all, I would like to express my immeasurable appreciation and deep sense of gratitude to my supervisor Dr. Georgios H. Vatistas for his full support, financial help, expert guidance, understanding and encouragement throughout my postgraduate studies and research. Without his continuous and incredible patience and counsel, the completion of my dissertation would not have been possible. I could not have imagined having a better mentor.

I would like to express my special thanks to my parents for supporting me not only during my studies, both graduate and postgraduate, but also throughout my whole life. Actually it is a lot more than just a thank you.

I am also deeply grateful to my sisters, Konstantina, Marianna, and Anastasia, my best friend Vicky and my friends Paris and Rahul for their emotional support these two years.

I would also like to extend my sincerest thanks to my favorite aunt Roula. She was always there for me and I will always appreciate the encouragement and the patience during my master studies.

Last but not least, I would like to confess my appreciation and love to my boyfriend, Dimitris, who always supports and motivates me.

Thesis Title:

New Solutions for Two-Cell Vortices

Table of Contents

List of Figures ..... **viii**

List of tables ..... **xi**

Nomenclature ..... **xii**

1. Introduction **1**

1.1 General 1

1.2 Literature review 5

1.3 Thesis contributions 16

2. Mathematical Formulation of the General Problem **17**

2.1 General formulation of incompressible intense vortices 17

2.2 General Formulation of Decaying Vortices 23

2.2.1 Transformation of steady vortices into time decay 23

2.2.2 The steady two-cell vortex 25

2.2.3 The decaying two-cell incompressible vortex formulation 27

2.3 The Steady-State Two-Cell Compressible Vortex 30

2.3.1 Simplification of mathematical problem 32

2.3.2 Numerical solution of the energy equation 37

3. Discussion of the Results 39

3.1 The Steady-State Two-Cell Incompressible Version of Vortex Model.....39

3.2 Time Decay of Two-Cell Vortices.....44

3.3 The Steady-State Two-Cell Compressible Version of the Vortex Model 50

3.3.1 Effect of Mach number on Temperature, Density and Pressure.....63

Conclusions.....67

Future Work.....69

References.....71

Appendix A.....77

Appendix B 99

List of Figures

Figure 1.1.1. The meridional (*r-z*) plane.....3

Figure 1.1.2. Flow pattern structure in *r-z* plane for one-cell vortices. (Credits: G.H.Vatistas).....3

Figure 1.1.3. Flow pattern structure in the *r-z* plane for two-cell vortices. (Credits: G.H.Vatistas).....4

Figure 1.2.1. Tangential velocity profile of Rankine's combined vortex compared to a variety of experimental vortices (adapted from Vatistas (2004)). 6

Figure 1.2.2. Vorticity profile for different vortex models.....7

Figure 1.2.3. Distribution of tangential velocity component for n-vortex profiles for different values of n (Credits: G.H.Vatistas).....10

Figure 2.1.1. Definition of coordinate system. 18

Figure 3.1.1. Comparison of the static pressure with the present two-cell incompressible vortex model and the experimental data of the Mulhall Tornado on 3 May 1999. (Discretized data from Lee and Wurman (2005)) 40

Figure 3.1.2. Comparison of the tangential velocity component with the present two-cell incompressible vortex model and the experimental data of the laboratory-simulated tornado. (Discretized data from Zhang and Sarkar (2008)). 41

Figure 3.1.3. Comparison of the tangential velocity component with the present two-cell incompressible vortex model and the experimental data of the Texas dust devil on 25 May 1999. (Discretized data from Bluestain et al. (2004)) 42
Figure 3.1.4. Comparison of the tangential velocity component with the present two-cell incompressible vortex model and the experimental data of aerodynamic vortices. (Discretized data from Snedeker (1972)).....43

Figure 3.2.1. Temporal distribution of velocity components during the decaying of two-celled vortices (a) tangential velocity, (b) radial velocity, and (c) axial velocity ($\kappa = 1.1$, $\beta_1 = 0.375$, $\beta_2 = 0.6$). 46
Figure 3.2.2. Distribution of maximum values for radius versus time 47
Figure 3.2.3. Distribution of maximum values for tangential velocity versus time 48
Figure 3.2.4. Distribution of the dissipation function for steady two - and one - cell .49

Figure 3.3.1. Variation of the dimensionless radial velocity vs. radius for $M_o = 0.6$, $\kappa = 1.1$, $\beta_1 = 0.375$, and $\beta_2 = 0.6$. 51
Figure 3.3.2. Variation of dimensionless axial velocity vs. radius for $M_o = 0.6$, $\kappa = 1.1$, $\beta_1 = 0.375$, and $\beta_2 = 0.6$. 52
Figure 3.3.3. Variation of dimensionless tangential velocity vs. radius for $M_o = 0.6$, $\kappa = 1.1$, $\beta_1 = 0.375$, and $\beta_2 = 0.6$. 53

Figure 3.3.4. Net effect of heating and cooling of fluid element due to viscous dissipation and fluid expansion respectively in a laminar compressible 2-cell vortex for M_o =0.6, Pr =2/3, $\kappa = 1.1$, $\beta_1 = 0.375$, and $\beta_2 = 0.6$. 55

Figure 3.3.5. Radial distribution of density (β) for M_o = 0.6, Pr =2/3, $\kappa = 1.1$, $\beta_1 = 0.375$, and $\beta_2 = 0.6$. 56

Figure 3.3.6. The plot of dimensionless pressure (Π) along the radial direction for M_o = 0.6, Pr =2/3, $\kappa = 1.1$, $\beta_1 = 0.375$, and $\beta_2 = 0.6$. 57

Figure 3.3.7. Radial distribution of temperature (Θ) for M_o = 0.6, $\kappa = 1.1$, $\beta_1 = 0.375$, and $\beta_2 = 0.6$. 59

Figure 3.3.8. Comparison of net effect of heating and cooling of fluid element due to viscous dissipation and fluid expansion respectively in a laminar compressible one- and 2-cell vortex for M_o =0.6, Pr =2/3, κ =1.1, β_1 =0.375, and β_2 =0.6. 61

Figure 3.3.9. Radial distribution of temperature (Θ) for different Mach numbers with Pr =2/3, $\kappa = 1.1$, $\beta_1 = 0.375$, and $\beta_2 = 0.6$. 63

Figure 3.3.10. Radial distribution of density for different Mach numbers, with Pr =2/3, $\kappa = 1.1$, $\beta_1 = 0.375$, and $\beta_2 = 0.6$. 64

Figure 3.3.11. The plot of dimensionless pressure of (p / p_∞) along the radial direction for different Mach numbers, with Pr =2/3, $\kappa = 1.1$, $\beta_1 = 0.375$, and $\beta_2 = 0.6$. 65

List of tables

Table 2.1.1. Typical values of the vortex Reynolds numbers (Vatistas (1998)) 21

Nomenclature

C	Arbitrary constant	
c_p	Heat capacity at constant pressure	Ws / KgK
c_v	Heat capacity at constant volume	Ws / KgK
r, z	Radial and axial coordinates	m
θ	Azimuthal coordinate	
r_c	Core radius	m
T	Static temperature	K
Q	Total velocity vector	m / s
V_r, V_θ, V_z	Radial, tangential and axial velocity components	m / s
$V_{\theta c}$	Maximum tangential velocity at the core	m / s
s	Specific entropy	KJ / KgK
q	Velocity vector	
n	Vortex exponent of the n - family	
k	Thermal conductivity	W / mK
R	Gas constant	KJ / KgK
p	Static pressure	Pa
t	Time	s
u	Dimensionless radial velocity component	$V_r / V_{\theta c}$
w	Dimensionless axial velocity component	$V_z / V_{\theta c}, \zeta h$

V	Normalized tangential velocity component	$V_\theta / V_{\theta c}$
Re	Vortex Reynolds number	$\rho_\infty V_{\theta c} r_c / \mu$
U	Normalized radial velocity component	
H	Normalized axial velocity component	
Pr	Prandtl number	$\mu c_p / k$
M_o	Vortex Mach number	$V_{\theta c} / \sqrt{\gamma R T_\infty}$
m	Exponential constant	
o	Order of magnitude	
b, g	Dummy variables	
f	$\xi^2 \left\{ \frac{d}{d\xi} \left(\frac{V}{\xi} \right) \right\}^2$	

Greek Letters

α	Scaling constant	
β	Dimensionless density	ρ / ρ_∞
β_1, β_2	Constant scaling parameters	
γ	Specific heat ratio	c_p / c_v
Γ_∞	Vortex circulation	m^2 / s
δ	Order of magnitude	
Δp	Static pressure change	$p - p_\infty$
ε	Scaling constant	
ζ	Dimensionless axial coordinate	z / r_c

η	Dimensionless variable (function of radius and time)	
Θ	Dimensionless static temperature	T / T_∞
κ	Scaling constant	
λ	Positive smallest root	$\alpha Re / 2$
μ	Dynamic viscosity	Kg / ms
ν	Kinematic viscosity	m^2 / s
ξ	Dimensionless radial coordinate	r / r_c
Π	Dimensionless static pressure	$p / \rho_\infty V^2{}_{\theta max}$
ρ	Density	Kg / m^3
σ	Scaling constant	
τ	Dimensionless time	vt / r_c^2
Φ	Viscous dissipation function	W / m^3
ψ	Scaling constant	
Ω_z	Vorticity	

Operators used

∂	Partial derivative	
d	Total derivative	
$\frac{D}{Dt}$	Material derivative	$\equiv \frac{\partial}{\partial t} + V_r \frac{\partial}{\partial r} + \frac{V_\theta}{r} \frac{\partial}{\partial \theta} + V_z \frac{\partial}{\partial z}$

∇^2	Laplacian	$\equiv \frac{\partial^2}{\partial r^2} + \frac{1}{r}\frac{\partial}{\partial r} + \frac{1}{r^2}\frac{\partial^2}{\partial \theta^2} + \frac{\partial^2}{\partial z^2}$

Subscripts

∞	Infinity
c	Vortex core
max	maximum value

1. Introduction

1.1 General

A vortex is understood to be the energetic rotation of gas, liquid, or plasma around a single center. Everyday paradigms include the swirling motion of coffee in a cup and the draining action of water in a bathtub. These also emerge in many other places in both the technological and the natural worlds. Vortices could appear in a variety of sizes, shapes, strengths, and last different lifetimes. They can be as small as the minuscule turbulent eddy to the enormous planetary vortices.

The impact of vortices on the overall flow development can be positive as well as negative. On one hand, in many industrial applications, such as for example in gas turbine combustors, vortex separators, incinerators, and heat exchangers these are important for the proper function of the machine. On the other hand, the appearance of vortices can generate unwanted aftereffects, such as the increase of the induced drag, in the case of trailing vortices in airplane wings, reducing their lift efficiency and breed very hazardous conditions. Moreover, these are known to generate vibration and noise. Engineers try to find ways to produce the first efficiently and weaken the second.

Strong atmospheric vortices like tornadoes, and tropical cyclones (hurricanes and typhoons) cause every year loss of life and considerable property damage. At the present, scientists are searching to find ways to detect these violent whirls soon enough so as to early warn inhabitants of the impending danger. Understanding the internal workings of vortices may help in finding ways in the future to possibly diminish their catastrophic damage.

In general, there are two idealized types of vortices: the free- (also known as potential) and the forced-vortex. In a free-vortex, the peripheral velocity reduces hyperbolically with the radius. In a forced-vortex the velocity increases linearly with the radius, or the vortex core $0 \le r \le r_c$ rotates if it were a solid body. The core radius (r_c) is that very close to the center of rotation where the tangential velocity reaches its maximum value.

Concentrated vortices are these where most of the vorticity lives inside the core. Intense or strong vortices are those where the radial and axial velocity components are neglected, as their values are considerably smaller as compared to the magnitude of the tangential. If the far-field fluid converges towards the center of rotation and then deflects upwards, then there is only a single recirculation zone present in the meridional *r-z*, (Fig. 1.1.1) plane, see Fig. 1.1.2. This type of vortex is known as one-cell. If there is a multitude of recirculation zones forming in the *r-z* plane then the vortex is multi-cell. A vortex of the two-cell kind is displayed in Fig. 1.1.3.

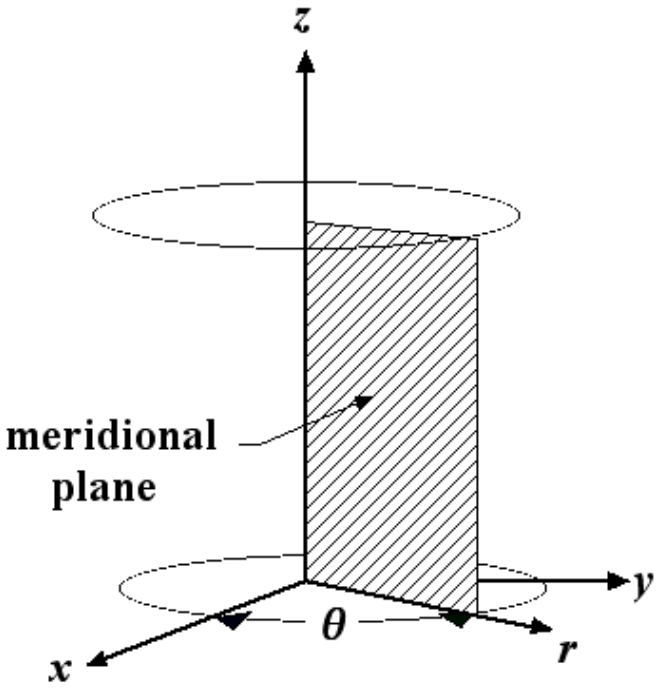

Figure 1.1.1. The meridional (*r*-*z*) plane.

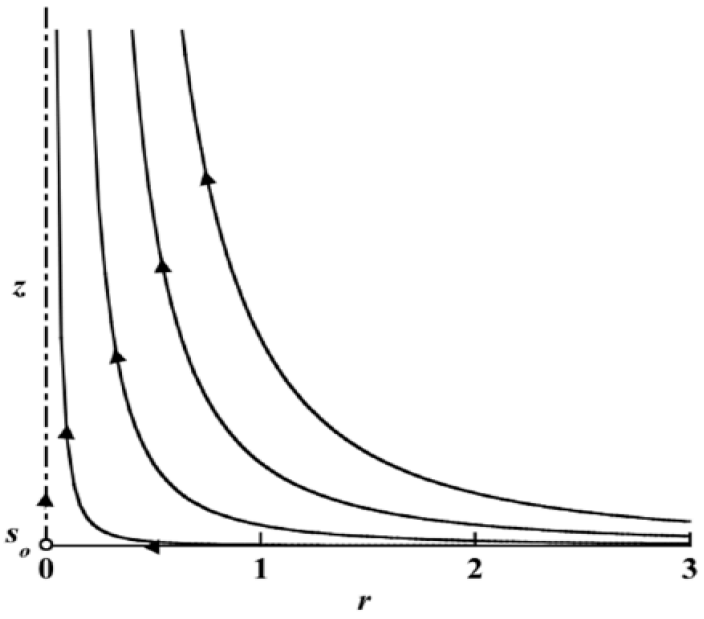

Figure 1.1.2. Flow pattern structure in *r*-*z* plane for one-cell vortices. (Credits: G.H.Vatistas)

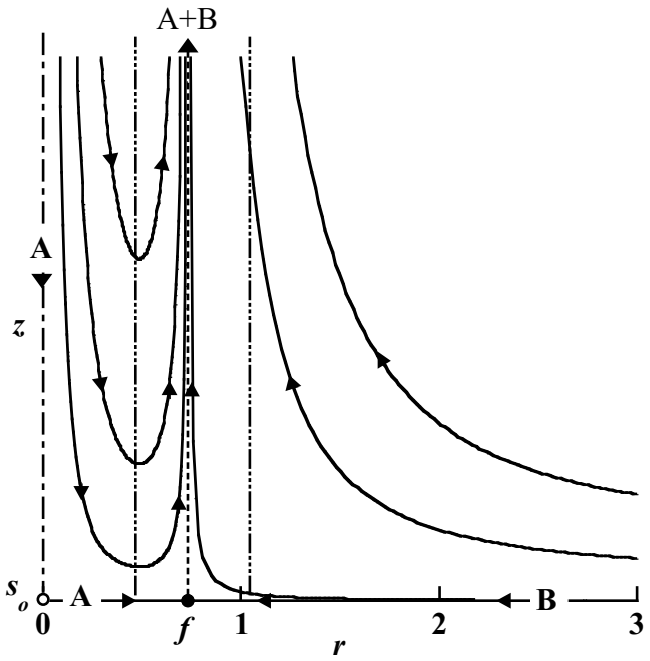

Figure 1.1.3. Flow pattern structure in the *r-z* plane for two-cell vortices. (Credits: G.H.Vatistas)

This vortex, as previously mentioned, is referred as two-cell because there are two secondary recirculating flow structures manifested in the meridional plane. Near the vortex axis the fluid descends (A) from above diverging outwards near the ground. The last stream collides with the incoming flow (B) of the outer compartment. Both streams (A+B) deflect upwards forming the two-cell fluid motion shown in Fig. 1.1.3.

1.2 Literature review

Although philosophical considerations of vortices started in antiquity, with amongst others Democritus's vortex atom (4th century BC) hypothesis and then at the end of renaissance (17th Century AD), with Descartes's Vortex Universe postulation, their epistemological study, as we know it now, began in the Victorian era (19th century AD). Helmoholtz (1858) and Rankine (1858) laid the foundations of the scientific study of vortices. Their contributions has since then produced an enormous amount of information *vis-à-vis* the event. In the initial stages, the studies were focused on incompressible steady one-cell vortices.

Helmhotz's (1858) research was based on the now renowned three theorems of vorticity. Rankine (1858), based on the vortex water-wheel vortex of Professor's James Thomson of Belfast (older brother of Lord Kelvin), presented the first mathematical vortex model, in which the tangential velocity component was only a function of radius and both radial and axial velocities were assumed to be zero. His formula considered a forced-vortex or solid body rotation inside the core $0 \le r \le r_c$ (linear tangential velocity distribution), and a free or potential vortex outside $r \ge r_c$,

Velocity distribution

$$V \propto \begin{cases} \xi \ \ for \quad \xi < 1 \\ 1/\xi \ for \quad \xi \geq 1 \end{cases} \tag{1.2.1}$$

In both modes (forced and free) the radial and axial velocity components are zero,

$$u = h = 0 \tag{1.2.2}$$

All the variables are defined in the nomenclature. Besides near the core, this formulation approximates very well the observed tangential velocity see Fig. 1.2.1.

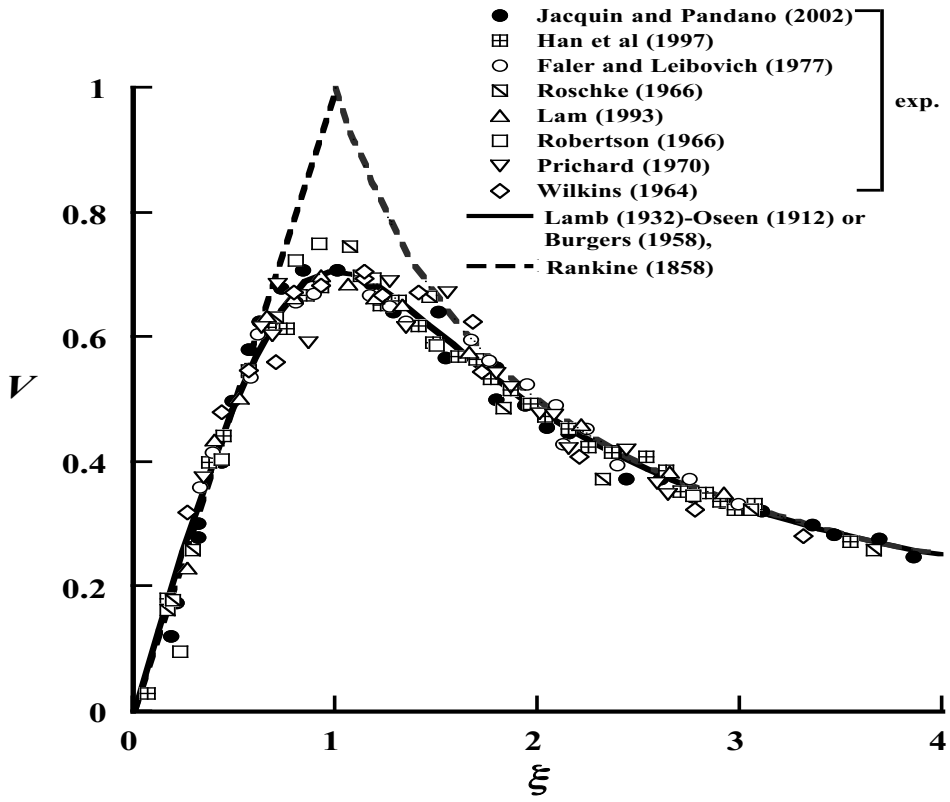

Figure 1.2.1. Tangential velocity profile of Rankine's combined vortex compared to a variety of experimental vortices (adapted from Vatistas (2004)).

However, Rankine's (1858) combined model posed several physical problems. At the point of transition ($r = r_c$), there is a discontinuity in vorticity (Ω_z),

$$\Omega_z = \frac{1}{\xi}\frac{d}{d\xi}(V\xi) \tag{1.2.3}$$

Specifically, within the core vorticity remains constant and becomes zero in the outer periphery through a jump discontinuity at $\xi = 1$ $(r = r_c)$, see Fig. 1.2.2. In real life however, as nature abhors discontinuities, this transition from forced vortex to potential vortex should be smooth.

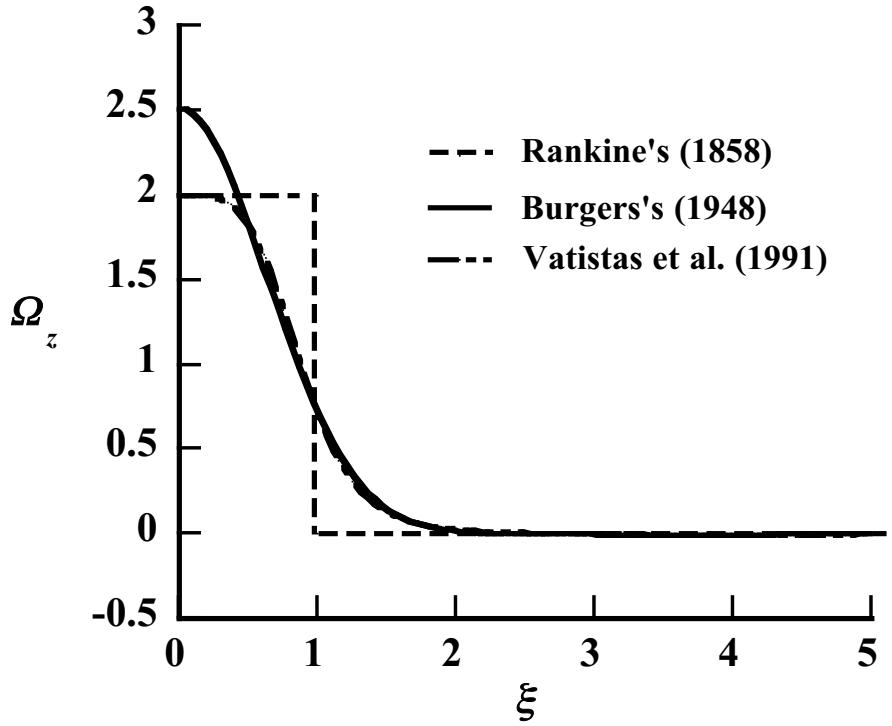

Figure 1.2.2. Vorticity profile for different vortex models

Burgers' (1948) proposed a way to smoothen the transition of vorticity. His model presupposed a linear radial velocity *u* variation:

$$u = -\frac{2\kappa}{\mathrm{Re}}\xi \tag{1.2.4}$$

which removed the sharp peak of the tangential velocity profile V at the core ($r = r_c$) see Fig. 1.2.3, thus removing the singularity in Ω_z (Fig. 1.2.2):

$$V = \frac{1}{\xi}\left[1 - exp(-\kappa\xi^2)\right] \tag{1.2.5}$$

The axial velocity is given by:

$$h = \frac{4\kappa}{\mathrm{Re}\,\xi} \tag{1.2.6}$$

where $\kappa = 1.2564$.

Burger's (1948) model correlates better with the experimental values of tangential velocity near the core as shown in Fig. 1.2.3. But, the radial velocity is unbounded, making it unsuitable for unconfined vortices. This formulation pertains also to one-cell vortex see the illustration of the flow in the *r-z* plane shown in Figure 1.1.2.

Vatistas et al. (1991) provided a new model that does not suffer from the previous impediments. The velocity components are given by:

Tangential velocity:

$$V = \frac{\xi}{\left(1+\xi^{2n}\right)^{\left(1/n\right)}} \tag{1.2.7}$$

Radial velocity:

$$u = \frac{-2\left(n+1\right)}{\mathrm{Re}} \frac{\xi^{\left(2n-1\right)}}{\left(1+\xi^{2n}\right)} \tag{1.2.8}$$

Axial velocity:

$$h = \frac{4n\left(n+1\right)}{\mathrm{Re}\cdot\zeta} \frac{\xi^{2\left(n-1\right)}}{\left(1+\xi^{2n}\right)^{2}} \tag{1.2.9}$$

Equations (1.2.8) and (1.2.9) are deducted from θ-momentum and continuity equation, respectively.

Depending on the choice of n, Vatistas' model can represent the velocity profiles that range from Rankine's (1858) to Scully's (1975) for $n = 1$. According to Ramesh et al. (2014) and many other investigators, the model with $n = 2$ provides an excellent approximation of Burger's (1948) (or Lamb (1932) - Oseen (1912)) vortex. This versatile, simple formulation has been adopted worldwide presently as the model to use for several studies of intense vortices by both academia and industry.

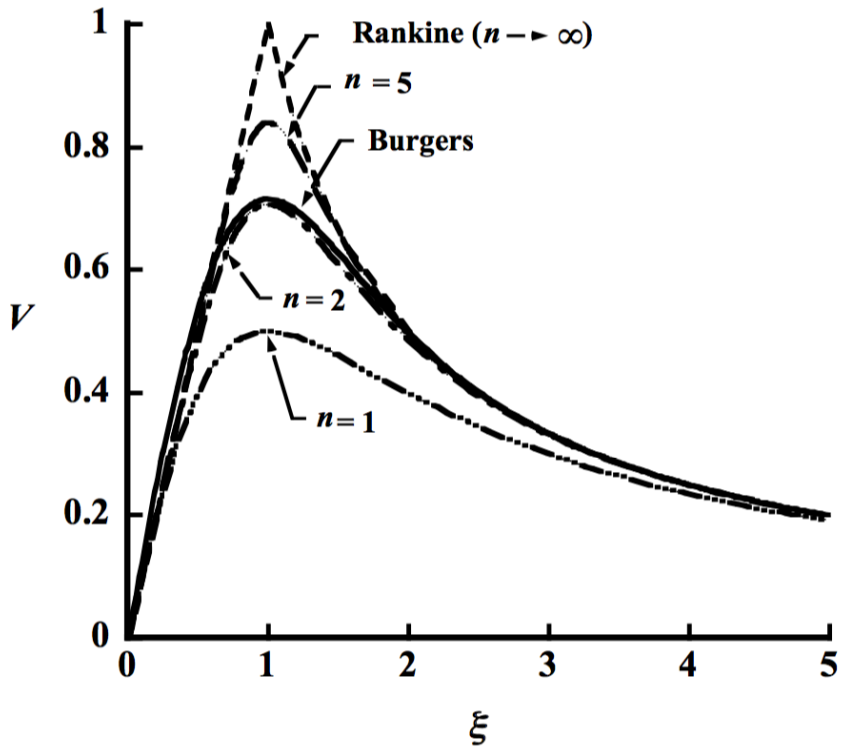

Figure 1.2.3. Distribution of tangential velocity component for n-vortex profiles for different values of n (Credits: G.H.Vatistas)

All the previously mentioned models pertained to single cell vortices. In 1959, Sullivan (1959) proposed a two-cell vortex archetype (see Figure 1.1.3). His formulation displays a reversal in flow direction in the radial and axial velocity components near the vortex center thus generating a central recirculation pattern that was absent in the previous one-cell vortices. Unfortunately, alike to Burger's vortex, the radial velocity grows without limits.

The velocity components in Sullivan's vortex are given by:

Tangential velocity,

$$V = \frac{1}{\xi}\frac{A\left(\varepsilon\xi^2\right)}{A\left(\infty\right)} \tag{1.2.10}$$

where $A\left(\varepsilon\xi^2\right) = \int_0^{\xi} g\, exp\left(-\int_0^{g}\left[-2\varepsilon b + \frac{6}{b}\left(1 - e^{-\varepsilon b^2}\right)\right]db\right)dg$ (1.2.11)

and

$$A\left(\infty\right) = \lim_{\xi\to\infty} A\left(\varepsilon\xi^2\right) \tag{1.2.12}$$

Radial velocity,

$$u = -2\varepsilon\xi + \frac{6}{\xi}\left(1 - e^{-\varepsilon\xi^2}\right) \tag{1.2.13}$$

Axial velocity,

$$h = -2\varepsilon\left(2 - 6e^{-\varepsilon\xi^2}\right) \tag{1.2.14}$$

In 1998, Vatistas (1998) proposed yet another simple vortex model for intense self-similar vortices. His generalized approach, depending on the choice of different values of scaling constants $\left(\alpha,\sigma,\kappa,\psi\right)$, could produce a single- or a double-celled intense vortex. The velocity components are given by:

Axial Velocity,

$$h = 2\alpha\left[\frac{1}{\left(1+\sigma\psi\xi^2\right)^2} - \frac{\kappa}{\left(1+\psi\xi^2\right)^2}\right] \tag{1.2.15}$$

Radial velocity,

$$u = \alpha\xi\left[\frac{\kappa}{1+\psi\xi^2} - \frac{1}{1+\sigma\psi\xi^2}\right] \tag{1.2.16}$$

Tangential velocity,

$$V = \frac{C}{\xi}\int_0^{\xi}\left[\frac{1+\psi\xi^2}{\left(1+\sigma\psi\xi^2\right)^{(1/\sigma\kappa)}}\right]^m \xi d\xi \tag{1.2.17}$$

Given the tangential velocity, Eqs. (1.2.15) and (1.2.16) are obtained from continuity and conservation of tangential momentum, respectively.

Recently, Israt Jahan Eshita (2014) extended the work of Vatistas (1998) to produce a formulation that is applicable to multi-celled incompressible vortices.

Most of the contributions in the scientific literature pertain to incompressible vortices. Nevertheless, it has been noted that in some instances the density variation cannot be ignored.

Several studies have been made on the topic of compressible swirling flows. In 1930, Taylor (1930) proposed a theoretical paper on isentropic potential vortex, which presented for the first time the impact of density variation in vortices. In the mid-1950's, many studies with respect to vortex/shockwave interplay came to light, such as those of Hollingsworth and Richards (1955) and Howard and Matthews (1956). Since then, a few contributions have been made with the most significant were the result of NASA's gaseous nuclear rocket motor (Ragsdale, 1960) and the refrigeration effect due to the temperature decrease in Ranque-Hilsh tube (Sibulkin, 1962).

On a different note, Meager (1961) examined analytically an isentropic swirling flow through a nozzle and he found an approximate solution. In 1959, Rott (1959) investigated the temperature profile in a steady Burger's vortex under limitative conditions. In 1960, Mack (1960) studied the laminar compressible vortex flow, generated inside a rotating cylinder. Subsequently, the radial flow was included in the approximate solution of Mack (1960) by Bellamy and Knights (1980). Sibulkin (1961) analyzed the decay of Taylor's vortex for low Mach number ($M << 1$). Brown (1965) extended the theory of Hall (1966) on three-dimensional vortices adding in the variable of density.

Later on, Colonius et al. (1991) investigated the effects of density on time-dependent unconfined vortices in consideration of heat transfer. Thereafter, Bagai and Leishman (1993) visualized under isentropic condition the helicopter blade vortices using the density gradient method. In the nineties, Chiocchia (1989) and Ardalan et

al. (1995) explored analytically via hodograph plane transformation the ideal compressible vortices.

Ellenrieder and Cantwell (2000) were embarked to inquire the self-similar compressible free vortices. Perez-Saborid et al. (2002) examined the development of unconfined vortices taking into consideration the thermal effects. Rusak and Lee (2004) studied the effects of density of vortex flow through a pipe, while studies on compressible tip vortices were made by Mandella (1987), Kalkhoran and Smart (2000), and Cattafest and Settles (1992).

In 2006, Vatistas and Aboelkassem (2006) extended the incompressible $n = 2$ model into compressible. All the governing equations were simplified, assuming strong vortices where all velocity components can be converted into a compressible via a proper variable transformation. Analytically, the pressure and density expressions were calculated from the equation of state and the radial momentum respectively. Furthermore, the temperature equation was obtained from the energy equation. From the three velocity components, only the tangential velocity was found to be independent of the density, while radial and axial velocity components were affected by changes in density.

Various experiments have shown that due to viscous effects, a vortex will decay in time. Oseen (1912), Hamel (1916) and Lamb (1932) considered the decay of a free vortex. In 2006, Vatistas and Aboelkassem (2006) proposed a new theoretical

methodology, concerning the similarities between steady and unsteady vortices. Their study showed that a steady-state vortex solution could be converted into time-dependent, and vice versa through a simple transformation of the dependent variables (Vatistas and Aboelkassem, 2006a).

1.3 Thesis contributions

In this thesis, two new solutions for two-cell vortices are presented. First, through the simple transformation (Vatistas and Aboelkassem, 2005), the time decaying version of the two-cell incompressible steady formulation is attained. Second, based on the work of Vatistas (1998) and Vatistas and Aboelkassem (2006) a new theoretical representation for laminar compressible two-celled vortices is derived.

2. Mathematical Formulation of the General Problem

2.1 General formulation of incompressible intense vortices

Here a time-dependent, incompressible, free of body forces, intense vortex is assumed. The mathematical representation of the problem include the following form of the conservation of mass (continuity) and momentum equations (Navier-Stokes) in cylindrical coordinates (Fig 2.1.1):

Continuity

$$\frac{\partial V_r}{\partial r} + \frac{V_r}{r} + \frac{\partial V_z}{\partial z} = 0 \qquad (2.1.1)$$

r-momentum

$$\rho\left\{\frac{\partial V_r}{\partial t} + V_r\frac{\partial V_r}{\partial r} + V_z\frac{\partial V_r}{\partial z} - \frac{V_\theta{}^2}{r}\right\} = -\frac{\partial \Delta p}{\partial r} + \mu\left\{\frac{\partial^2 V_r}{\partial r^2} + \frac{1}{r}\frac{\partial V_r}{\partial r} - \frac{V_r}{r^2} + \frac{\partial^2 V_r}{\partial z^2}\right\} \qquad (2.1.2)$$

z - momentum

$$\rho\left\{\frac{\partial V_z}{\partial t} + V_r\frac{\partial V_z}{\partial r} + V_z\frac{\partial V_z}{\partial z}\right\} = -\frac{\partial \Delta p}{\partial z} + \mu\left\{\frac{\partial^2 V_z}{\partial r^2} + \frac{1}{r}\frac{\partial V_z}{\partial r} + \frac{\partial^2 V_z}{\partial z^2}\right\} \qquad (2.1.3)$$

θ-momentum

$$\rho\left\{\frac{\partial V_\theta}{\partial t}+V_r\frac{\partial V_\theta}{\partial r}+V_z\frac{\partial V_\theta}{\partial z}+\frac{V_rV_\theta}{r}\right\}=\mu\left\{\frac{\partial^2 V_\theta}{\partial r^2}+\frac{1}{r}\frac{\partial V_\theta}{\partial r}-\frac{V_\theta}{r^2}+\frac{\partial^2 V_\theta}{\partial z^2}\right\} \qquad (2.1.4)$$

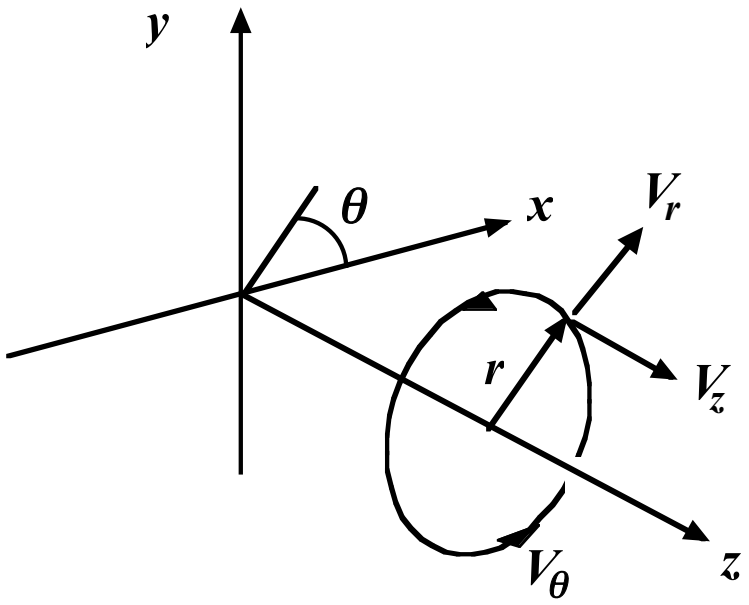

Figure 2.1.1. Definition of coordinate system.

Using the dimensionless form of the variables, as in Aboelkassem and Vatistas (2007),

$$\xi = r / r_c$$

$$\zeta = z / r_c$$

$$u = V_r / V_{\theta c}$$

$$w = V_z / V_{\theta c} = \zeta h$$

$$V = V_\theta / V_{\theta c}$$

$$V_{\theta c} = \Gamma_\infty / 2\pi r_c$$

$$\Delta p = p - p_\infty$$

$$\Pi = \Delta p / \rho_\infty V^2{}_{\theta c}$$

$$Re = \rho_\infty V_{\theta c} r_c / \mu$$

where subscript "c" identifies properties at the vortex core (defined as the radius where the tangential velocity attains its maximum), the governing equations take the following form:

We assume a steady vortex flow and based on the previous dimensionless form, the governing equations are:

Continuity

$$\frac{\partial u}{\partial \xi} + \frac{u}{\xi} + h = 0 \tag{2.1.5}$$

$\delta \quad \delta \quad \delta$

r-momentum

$$Re\left\{u\frac{\partial u}{\partial \xi} - \frac{V^2}{\xi}\right\} = -Re\frac{\partial \Pi}{\partial \xi} + \frac{\partial^2 u}{\partial \xi^2} + \frac{1}{\xi}\frac{\partial u}{\partial \xi} - \frac{u}{\xi^2} \tag{2.1.6}$$

$1/\delta \ (\delta\delta \quad 1) \quad (1/\delta)\delta \quad \delta \quad \delta \quad \delta$

z-momentum

$$Re\left\{u\frac{\partial h}{\partial \xi} + h^2\right\} = -\frac{Re}{\xi}\frac{\partial \Pi}{\partial \zeta} + \frac{\partial^2 h}{\partial \xi^2} + \frac{1}{\xi}\frac{\partial h}{\partial \xi} \tag{2.1.7}$$

$1/\delta \ (\delta\delta \quad \delta^2) \quad (1/\delta)\delta \quad \delta \quad \delta$

θ-momentum

$$Re\left\{u\frac{\partial V}{\partial \xi} + \frac{Vu}{\xi}\right\} = \frac{\partial^2 V}{\partial \xi^2} + \frac{1}{\xi}\frac{\partial V}{\partial \xi} - \frac{V}{\xi^2} \tag{2.1.8}$$

$1/\delta \ (\delta 1 \quad 1\delta) \quad 1 \quad 1 \quad 1$

In the present study we are interested in solutions in strong vortices where the radial (u) and axial (h) velocity components are substantially weaker than the tangential (V). According to the Table 2.1.1, δ represents a very small number with order of magnitude ranging from 10^{-5} to 10^{-7} (Vatistas, 1998).

Table 2.1.1. Typical values of the vortex Reynolds numbers (Vatistas (1998))

Type of vortex	r_c (m)	$V_{\theta\,\max}$ (m/s)	Re	δ
Tornadoes	10.0	60.0	$4.0\ 10^7$	o (10^{-7})
Dust devils	3.0	10.0	$5.0\ 10^6$	o (10^{-6})
Whirl pools	15.0	5.0	$7.5\ 10^7$	o (10^{-7})
Cyclone chamber and wing tip vortices	0.2	0.5	$6.7\ 10^5$	o (10^{-5})
Bath tub vortices	0.2	0.1	$2.0\ 10^4$	o (10^{-4})
Aerodynamic	1.0	10.0	$6.7\ 10^5$	o (10^{-5})

Neglecting terms of δ or smaller magnitude the above equations are reduced into:

Continuity:

$$\frac{du}{d\xi} + \frac{u}{\xi} + h = 0 \tag{2.1.9}$$

r- momentum:

$$\frac{V^2}{\xi} = \frac{d\Pi}{d\xi} \tag{2.1.10}$$

z - momentum:

$$\frac{d\Pi}{d\zeta} = 0 \tag{2.1.11}$$

The equation of axial momentum equation (Eq. 2.1.11) shows that the dimensionless static pressure does not vary in the axial direction ζ (from the axisymmetric condition $\Pi \neq fn(\theta)$). Therefore, the pressure must be a sole function of ξ, or,

Tangential θ-momentum:

$$\frac{u}{\xi}\frac{d(\xi V)}{d\xi} = \frac{1}{Re}\frac{d}{d\xi}\left\{\frac{1}{\xi}\frac{d}{d\xi}(\xi V)\right\} \tag{2.1.12}$$

In addition to the field equations, appropriate boundary conditions are required for a proper definition of the problem. These are:

(i) $\xi = 0, \quad V = u = 0$ and $\frac{dh}{d\xi} = 0$

(ii) $\xi \to \infty, \quad V \cdot \xi \to 1$

2.2 General Formulation of Decaying Vortices

2.2.1 Transformation of steady vortices into time decay

For a decaying vortex the velocity vector is given by:

$$V = \{u(\tau,\xi), V(\tau,\xi), w(\tau,\xi) = \zeta h(\tau,\xi)\} \tag{2.2.1}$$

Continuity and the Navier-Stokes equations for this problem are the same as before, Eqs. (2.1.5)- (2.1.7). However, it must be understood that in addition to the radius (ξ) u and h are also functions of time (τ). The θ-momentum equation is given by:

$$\frac{\partial V}{\partial \tau} + \frac{u}{\xi}\frac{\partial(\xi V)}{\partial \xi} = \frac{1}{Re}\frac{\partial}{\partial \xi}\left\{\frac{1}{\xi}\frac{\partial(\xi V)}{\partial \xi}\right\} \tag{2.2.2}$$

The above system is underdetermined as the number of unknowns (u, h, V, Π) and equations Eqs. (2.1.5), (2.1.6) and (2.1.7) is not the same.

Here, in order to close the system of equations a realistic tangential velocity is assumed and the rest of the parameters are determined using Eqs. (2.2.2), (2.1.5) and (2.1.6).

Using the following dependent variable transformations:

$$\eta=\xi/\sqrt{1+\tau} \quad \text{(a)} \qquad V(\eta)=V(\tau,\xi)\sqrt{1+\tau} \quad \text{(b)}$$

$$U(\eta)=u(\tau,\xi)Re\sqrt{1+\tau}-\frac{\eta}{2} \quad \text{(c)} \qquad \Delta\Pi=(1+\tau)p(\tau,\xi) \quad \text{(d)}$$

$$H(\eta)=1+h(\tau,\xi)Re(1+\tau) \quad \text{(e)} \qquad (2.2.3)$$

These equations can be transformed into the ordinary set:

$$\frac{dU}{d\eta}+\frac{U}{\eta}+H(\eta)=0 \qquad (2.2.4)$$

$$\frac{V^2(\eta)}{\eta}=\frac{d\Delta\Pi}{d\eta} \qquad (2.2.5)$$

$$\frac{U(\eta)}{\eta}(V\eta)'=V''+\frac{1}{\eta}V'-\frac{V}{\eta^2} \qquad (2.2.6)$$

In addition to the field equations, appropriate boundary conditions are required for a proper definition of the problem. These are:

(iii) $\eta=0, \quad V=U=0$ and $\frac{dH}{d\xi}=0$

(iv) $\eta\to\infty, \quad V\cdot\eta\to 1$

All the details are provided in Appendix A. The equations of the above system is represented by similar equations as the steady-state version.

2.2.2 The steady two-cell vortex

In this dissertation, the model of Vatistas (1998) is used in order to simulate two-celled intense self-similar steady vortices. These are:

Axial velocity:

$$h = 2\lambda\left[\frac{1}{\left(1+\beta_1\xi^2\right)^2} - \frac{\kappa}{\left(1+\beta_2\xi^2\right)^2}\right] \tag{2.2.7}$$

where κ, β_1, β_2 and λ are scaling constants.

Based on conservation of mass (Eq. (2.1.5)) the radial velocity component is obtained,

Radial velocity:

$$u = -\lambda\left[\frac{\xi}{1+\beta_1\xi^2} - \frac{\kappa\xi}{1+\beta_2\xi^2}\right] \tag{2.2.8}$$

The tangential velocity component is obtained by inserting the radial velocity equation into the θ-momentum Eq. (2.1.8). After a double integration and applying the boundary condition $V\cdot\xi \to 1$ as $\xi \to \infty$, the general form of the tangential velocity is obtained:

$$V = \frac{1}{\xi} \frac{\int_0^{\xi} \left[\frac{\left(1+\beta_2\xi^2\right)^{\frac{\kappa}{2\beta_2}}}{\left(1+\beta_1\xi^2\right)^{\frac{1}{2\beta_1}}} \right]^{\lambda} \xi\, d\xi}{\int_0^{1} \left[\frac{\left(1+\beta_2\xi^2\right)^{\frac{\kappa}{2\beta_2}}}{\left(1+\beta_1\xi^2\right)^{\frac{1}{2\beta_1}}} \right]^{\lambda} \xi\, d\xi} \qquad (2.2.9)$$

However, there is one more requirement that should be satisfied by the velocity profile: the maximum velocity must occur at $\xi = 1$. Therefore, from the Eq. (2.2.9), the following equation is derived:

$$\left[\frac{\left(1+\beta_2\xi^2\right)^{\frac{\kappa}{2\beta_2}}}{\left(1+\beta_1\xi^2\right)^{\frac{1}{2\beta_1}}} \right]^{\lambda} - \int_0^{1} \left[\frac{\left(1+\beta_2\xi^2\right)^{\frac{\kappa}{2\beta_2}}}{\left(1+\beta_1\xi^2\right)^{\frac{1}{2\beta_1}}} \right]^{\lambda} \xi\, d\xi = 0 \qquad (2.2.10)$$

The value of the root (λ) is found numerically by solving the Eq. (2.2.10) with the help of Matlab software.

2.2.3 The decaying two-cell incompressible vortex formulation

For our case the two cell steady solution is:

$$V = \frac{1}{\xi} \frac{\int_0^{\xi} \left[\frac{\left(1+\beta_2 \xi^2\right)^{\frac{\kappa}{2\beta_2}}}{\left(1+\beta_1 \xi^2\right)^{\frac{1}{2\beta_1}}} \right]^{\lambda} \xi d\xi}{Y(\infty)} \tag{2.2.11}$$

$$\text{where } Y(\infty) = \int_0^1 \left[\frac{\left(1+\beta_2 \xi^2\right)^{\frac{\kappa}{2\beta_2}}}{\left(1+\beta_1 \xi^2\right)^{\frac{1}{2\beta_1}}} \right]^{\lambda} \xi \, d\xi \tag{2.2.12}$$

In order to transform this into decaying vortex we replace on the right hand side ξ by

$$\eta = \frac{\xi}{\sqrt{1+\tau}} \tag{2.2.13}$$

Therefore, we take the following equation for tangential velocity:

$$V(\eta) = \frac{1}{\eta} \frac{\int_0^{\eta} \left[\frac{\left(1+\beta_2 \eta^2\right)^{\frac{\kappa}{2\beta_2}}}{\left(1+\beta_1 \eta^2\right)^{\frac{1}{2\beta_1}}} \right]^{\lambda} \eta d\eta}{Y(\infty)} \tag{2.2.14}$$

On the left hand side we have,

$$V(\eta) = V(\tau, \xi) \sqrt{1+\tau} \tag{2.2.15}$$

Then, inserting Eq. (2.2.15) into Eq. (2.2.14), yields:

$$V(\tau,\xi)\sqrt{1+\tau}=\frac{1}{\frac{\xi}{\sqrt{1+\tau}}}\frac{\int_0^{\eta}\left[\frac{\left(1+\beta_2\eta^2\right)^{\frac{\kappa}{2\beta_2}}}{\left(1+\beta_1\eta^2\right)^{\frac{1}{2\beta_1}}}\right]^{\lambda}\eta d\eta}{Y(\infty)} \tag{2.2.16}$$

or

$$V(\tau,\xi)=\frac{1}{\frac{\xi}{\sqrt{1+\tau}}\sqrt{1+\tau}}\frac{\int_0^{\frac{\xi}{\sqrt{1+\tau}}}\left[\frac{\left(1+\beta_2\left[\frac{\xi}{\sqrt{1+\tau}}\right]^2\right)^{\frac{\kappa}{2\beta_2}}}{\left(1+\beta_1\left[\frac{\xi}{\sqrt{1+\tau}}\right]^2\right)^{\frac{1}{2\beta_1}}}\right]^{\lambda}\frac{\xi}{\sqrt{1+\tau}}d\left(\frac{\xi}{\sqrt{1+\tau}}\right)}{Y(\infty)} \tag{2.2.17}$$

Finally, the tangential velocity becomes,

$$V(\tau,\xi)=\frac{1}{\xi(1+\tau)}\frac{\int_0^{\frac{\xi}{\sqrt{1+\tau}}}\left[\frac{\left(1+\beta_2\left[\frac{\xi}{\sqrt{1+\tau}}\right]^2\right)^{\frac{\kappa}{2\beta_2}}}{\left(1+\beta_1\left[\frac{\xi}{\sqrt{1+\tau}}\right]^2\right)^{\frac{1}{2\beta_1}}}\right]^{\lambda}\xi d\xi}{Y(\infty)} \tag{2.2.18}$$

The radial and axial velocity components are obtained using the procedure described in Appendix A.

Radial velocity

$$u(\tau,\xi)Re=\frac{\xi}{1+\tau}\left\{\frac{1}{2}-\left(\frac{1}{1+\beta_1\frac{\xi^2}{1+\tau}}-\frac{\kappa}{1+\beta_2\frac{\xi^2}{1+\tau}}\right)\lambda\right\} \tag{2.2.19}$$

Axial velocity

$$h(\tau,\xi)Re=\frac{1}{1+\tau}\left\{\left(\frac{1}{\left(1+\beta_1\frac{\xi^2}{1+\tau}\right)^2}-\frac{\kappa}{\left(1+\beta_2\frac{\xi^2}{1+\tau}\right)^2}\right)2\lambda-1\right\} \tag{2.2.20}$$

These equations will be used to study the decay of double-cell vortices in section.

2.3 The Steady-State Two-Cell Compressible Vortex

Let us now consider a compressible, axisymmetric, steady, swirling flow of a calorically perfect gas. The basic equations that are required to mathematically model the flow are, once more, the conservation of mass and momentum. Since the density is also a variable then conservation of energy is also to be included. By doing so an additional variable, namely the temperature, is introduced. For this reason, the equation of state must also be included to close the thermodynamics portion of the system.

Therefore, the equations describing the flow are:

Conservation of mass

$$\frac{\partial(\rho V_r)}{\partial r} + \frac{\rho V_r}{r} + \frac{\partial(\rho V_z)}{\partial z} = 0 \tag{2.3.1}$$

r-momentum

$$\rho\left\{V_r \frac{\partial V_r}{\partial r} - \frac{V_\theta{}^2}{r}\right\} = -\frac{\partial p}{\partial r} + \mu\left\{\frac{\partial^2 V_r}{\partial r^2} + \frac{1}{r}\frac{\partial V_r}{\partial r} - \frac{V_r}{r^2} + \frac{1}{3}\frac{\partial}{\partial r}\left(\frac{\partial V_r}{\partial r} + \frac{\partial V_z}{\partial z} + \frac{V_r}{r}\right)\right\} \tag{2.3.2}$$

θ-momentum

$$\rho\left\{V_r\frac{\partial V_\theta}{\partial r}+\frac{V_r V_\theta}{r}\right\}=\mu\left\{\frac{\partial^2 V_\theta}{\partial r^2}+\frac{1}{r}\frac{\partial V_\theta}{\partial r}-\frac{V_\theta}{r^2}\right\} \tag{2.3.3}$$

z-momentum

$$\rho\left\{V_r\frac{\partial V_z}{\partial r}+V_z\frac{\partial V_z}{\partial z}\right\}=-\frac{\partial p}{\partial z}+\mu\left\{\frac{\partial^2 V_z}{\partial r^2}+\frac{1}{r}\frac{\partial V_z}{\partial r}+\frac{\partial^2 V_z}{\partial z^2}+\frac{1}{3}\frac{\partial}{\partial r}\left(\frac{\partial V_r}{\partial r}+\frac{\partial V_z}{\partial z}+\frac{V_r}{r}\right)\right\}$$

(2.3.4)

Energy equation

$$\frac{1}{r}\frac{\partial}{\partial r}\left(kr\frac{\partial T}{\partial r}\right)+\frac{\partial}{\partial z}\left(k\frac{\partial T}{\partial z}\right)+\Phi=\rho\left(V_r\frac{\partial T}{\partial r}+V_z\frac{\partial T}{\partial z}\right)-\left(V_r\frac{\partial p}{\partial r}+V_z\frac{\partial p}{\partial z}\right) \tag{2.3.5}$$

where

$$\Phi=2\mu\left[\left(\frac{\partial V_r}{\partial r}\right)^2+\left(\frac{1}{r}\frac{\partial V_\theta}{\partial\theta}+\frac{V_r}{r}\right)^2+\left(\frac{\partial V_z}{\partial z}\right)^2+\frac{1}{2}\left(\frac{\partial V_\theta}{\partial r}-\frac{V_\theta}{r}+\frac{1}{r}\frac{\partial V_r}{\partial\theta}\right)^2\right.$$

$$\left.+\frac{1}{2}\left(\frac{1}{r}\frac{\partial V_z}{\partial\theta}+\frac{\partial V_\theta}{\partial z}\right)^2+\frac{1}{2}\left(\frac{\partial V_r}{\partial z}+\frac{V_r}{r}\right)^2-\frac{1}{3}(\nabla\cdot q)^2\right]$$

(2.3.6)

$$\nabla\cdot q=\frac{\partial V_r}{\partial r}+\frac{V_r}{r}+\frac{\partial V_z}{\partial z} \tag{2.3.7}$$

Equation of state:

$$p = \rho RT \tag{2.3.8}$$

The general form of the total velocity is defined as (Vatistas and Aboelkassem, 2006a):

$$\mathbf{q}\left[V_r(r), V_\theta(r), V_z = zfn(r)\right] \tag{2.3.9}$$

All the variables are specified in the nomenclature and the coordinate system is illustrated in Figure 2.1.1.

2.3.1 Simplification of mathematical problem

Using the dimensionless form of the variables mentioned in the subsection 2.1, and assuming that in intense vortices both radial and axial velocity components are very small (order of magnitude of δ Table 2.1.1.), the governing equations are transformed to the following dimensionless form:

Conservation of mass

$$\frac{\partial(\beta u)}{\partial \xi} + \frac{\beta u}{\xi} + \beta h = 0 \tag{2.3.10}$$

$\delta \quad \delta \quad \delta$

r-momentum

$$u\frac{\partial u}{\partial \xi}-\frac{V^2}{\xi}=-\frac{1}{\beta}\frac{\partial \Pi}{\partial \xi}+\frac{1}{Re\,\beta}\left[\frac{4}{3}\left(\frac{\partial^2 u}{\partial \xi^2}+\frac{1}{\xi}\frac{\partial u}{\partial \xi}-\frac{u}{\xi^2}\right)+\frac{1}{3}\frac{\partial^2(h\zeta)}{\partial \zeta \partial \xi}\right] \tag{2.3.11}$$

$(\delta\,\delta \quad 1)$ $\quad 1 \quad \delta \quad \delta \quad \delta \quad \delta \quad \delta$

Neglecting the terms of order δ or smaller yields:

$$\frac{\partial \Pi}{\partial \xi}=\frac{\beta V^2}{\xi} \tag{2.3.12}$$

θ-momentum

$$Re\,\beta\left\{u\frac{\partial V}{\partial \xi}+\frac{Vu}{\xi}\right\}=\frac{\partial^2 V}{\partial \xi^2}+\frac{1}{\xi}\frac{\partial V}{\partial \xi}-\frac{V}{\xi^2} \tag{2.3.13}$$

$1/\delta \quad (\delta 1 \quad 1\delta) \quad 1 \quad 1 \quad 1$

z-momentum

$$u\frac{\partial(\zeta h)}{\partial \xi}+\zeta h^2=-\frac{1}{\beta}\frac{\partial \Pi}{\partial \zeta}+\frac{1}{Re\,\beta}\left[\frac{\partial^2(\zeta h)}{\partial \xi^2}+\frac{1}{\xi}\frac{\partial(\zeta h)}{\partial \xi}+\frac{\partial^2(\zeta h)}{\partial \zeta^2}+\frac{1}{3}\frac{\partial}{\partial \zeta}\left(\frac{\partial u}{\partial \xi}+h+\frac{u}{\xi}\right)\right]$$

$(\delta\,\delta \quad \delta^2)$ $\quad 1 \quad \delta \quad \delta \quad \delta \quad \delta \quad \delta \quad \delta \quad \delta$

(2.3.14)

Neglecting the terms of δ or smaller magnitude and simplifying the above equation is reduced into:

$$\frac{\partial \Pi}{\partial \zeta} \approx 0 \tag{2.3.15}$$

We note that, as previously the dimensionless static pressure should not vary in the ζ-direction; therefore the pressure must be only a function of ξ. As a result, the partial derivative in Eq. (2.3.12), is transformed into total or,

$$\frac{d\Pi}{d\xi} = \frac{\beta V^2}{\xi} \tag{2.3.16}$$

State equation

$$\Pi = \frac{\beta \Theta}{\gamma M_o^2} \tag{2.3.17}$$

$1\ 1$

In addition, from the r-momentum, the density must also depend on ξ from Eq. (2.3.17); the temperature must also be sole function of ξ.

Energy equation

$$\frac{k\mathrm{T}_\infty}{r_c^2 \xi}\frac{d}{d\xi}\left(\xi \frac{d\Theta}{d\xi}\right) + \frac{d^2\Theta}{d\zeta^2} + \Phi = \beta \,\mathrm{Pr}\,\mathrm{Re}\left(\frac{k\mathrm{T}_\infty}{r_c^2}\right)\left(u\frac{d\Theta}{d\xi} + w\frac{d\Theta}{d\zeta}\right) - \frac{k\mathrm{T}_\infty}{r_c^2}\,\mathrm{Pr}\,\mathrm{Re}\left(\gamma - 1\right)M_o^2\left(u\frac{d\Pi}{d\xi} + w\frac{d\Pi}{d\zeta}\right)$$

$$1 \quad 1 \quad \delta\ \frac{1}{\delta} \quad \delta\ 1 \quad \delta\ 1 \quad \delta\ \frac{1}{\delta} \quad \delta \quad \delta$$

(2.3.18)

Using the order of magnitude, the dissipation function is:

$$\Phi = 2\mu\left[\left(\frac{V_{\theta c}}{r_c}\right)^2\left(\frac{\partial u}{\partial \xi}\right)^2 + \left(\frac{V_{\theta c}}{r_c}\right)^2\left(\frac{u}{\xi}\right)^2 + \left(\frac{V_{\theta c}}{r_c}\right)^2 (h)^2 + \frac{1}{2}\left(\frac{V_{\theta c}}{r_c}\right)^2\left(\frac{\partial V}{\partial \xi} - \frac{V}{\xi}\right)^2\right.$$

$$\delta^2 \qquad \delta^2 \qquad \delta^2 \qquad 1 \quad 1$$

$$\left. + \frac{1}{2}\left(\frac{V_{\theta c}}{r_c}\right)^2 \zeta^2\left(\frac{\partial h}{\partial \xi}\right)^2 - \frac{1}{3}\left(\frac{V_{\theta c}}{r_c}\right)^2\left(\frac{\partial u}{\partial \xi} + h + \frac{u}{\xi}\right)^2\right]$$

$$\delta^2 \qquad \delta^2 \qquad (2.3.19)$$

Neglecting terms of δ or higher yields:

$$\Phi = \mu\left(\frac{V_{\theta c}}{r_c}\right)^2\left(\frac{dV}{d\xi} - \frac{V}{\xi}\right)^2 \qquad (2.3.20)$$

$$\Phi = \Pr M_o^2(\gamma - 1)\left(\frac{k\mathrm{T}_\infty}{r_c^2}\right)\left[\xi^2\left\{\frac{d}{d\xi}\left(\frac{V}{\xi}\right)\right\}^2\right] \qquad (2.3.21)$$

Finally, the dissipation function becomes:

$$\Phi = Pr\, M_o^2(\gamma - 1)\left(\frac{kT_\infty}{r_c^2}\right) f \qquad (2.3.22)$$

where,

$$f = \left[\xi^2\left\{\frac{d}{d\xi}\left(\frac{V}{\xi}\right)\right\}^2\right]$$

Inserting the above expressions of Φ and $\frac{d\Pi}{d\xi}$ in Eq. (2.3.18) gives,

$$\frac{1}{\xi}\frac{d}{d\xi}\left(\xi\frac{d\Theta}{d\xi}\right)+Pr\,M_o^2(\gamma-1)f=\beta\,Pr\,Re\,u\frac{d\Theta}{d\xi}-Pr\,Re(\gamma-1)M_o^2u\frac{\beta V^2}{\xi} \tag{2.3.23}$$

Taking $U=\beta\,Re\,u$ (2.3.24)

and $H=\beta\,Re\,h$ (2.3.25)

Based on Eqs. (2.2.24) and (2.2.35), the governing equation and the equation of state are transformed to the following:

Conservation of mass:

$$\frac{1}{\xi}\frac{d}{d\xi}(U\xi)+H=0 \tag{2.3.26}$$

r-momentum

$$\frac{d\Pi}{d\xi}=\frac{\beta V^2}{\xi} \tag{2.3.27}$$

θ-momentum

$$\frac{U}{\xi}\frac{d}{d\xi}(V\xi)=\frac{d}{d\xi}\left[\frac{1}{\xi}\frac{d}{d\xi}(V\xi)\right] \tag{2.3.28}$$

Energy equation

$$\frac{1}{\xi}\frac{d}{d\xi}\left(\xi\frac{d\Theta}{d\xi}\right)-PrU\frac{d\Theta}{d\xi}=-Pr(\gamma-1)M_o^2\left(f+\frac{UV^2}{\xi}\right) \tag{2.3.29}$$

Equation of state

$$\Pi=\frac{\beta\Theta}{\gamma M_o^2} \tag{2.3.30}$$

Boundary conditions

The boundaries conditions for the problem are:

(i) $\xi=0$ $\qquad V=0,U=0,\frac{d\Theta}{d\xi}=0,\frac{dH}{d\xi}=0$

(ii) $\xi\to\infty$ $\qquad \left(V\cdot\xi,\Theta,\beta,\gamma M_o^2\Pi\right)\to 1$

2.3.2 Numerical solution of the energy equation

In the subsection 2.2.2, the general equations, which describe a two-cell family of vortices, were provided along with required boundary conditions. Based on the velocity components given by Eqs. (2.2.7), (2.2.8) and (2.2.9), the temperature will be obtained using the energy equation (Eq. (2.3.29)).

Inserting the equation for V (Eq. (2.2.9)) and U (Eqs. (2.2.8) and (2.3.24)) into the energy equation and integrating twice along with the boundary conditions, yields the temperature. After some straightforward mathematical manipulations, the temperature equation takes the following form:

$$\Theta = -\Pr(\gamma-1)M^2{}_o\int_0^{\xi}\left\{\frac{\left(1+\beta_2 g^2\right)^{\frac{Pr\,\kappa}{2\beta_2}}}{\left(1+\beta_1 g^2\right)^{\frac{Pr}{2\beta_1}}\,g}\int_0^{g}\frac{\left(1+\beta_1 b^2\right)^{\frac{Pr}{2\beta_1}}}{\left(1+\beta_2 b^2\right)^{\frac{Pr\,\kappa}{2\beta_2}}}\left(U(b)V(b)^2+bf(b)\right)db\right\}dg$$

$$+\Pr(\gamma-1)M^2{}_o\int_0^{\infty}\left\{\frac{\left(1+\beta_2 g^2\right)^{\frac{Pr\,\kappa}{2\beta_2}}}{\left(1+\beta_1 g^2\right)^{\frac{Pr}{2\beta_1}}\,g}\int_0^{g}\frac{\left(1+\beta_1 b^2\right)^{\frac{Pr}{2\beta_1}}}{\left(1+\beta_2 b^2\right)^{\frac{Pr\,\kappa}{2\beta_2}}}\left(U(b)V(b)^2+bf(b)\right)db\right\}dg+1 \qquad (2.3.31)$$

The details of the derivations are given in Appendix A.

3. Discussion of the Results

3.1 The Steady-State Two-Cell Incompressible Version of Vortex Model

In this chapter, a sample of correlations of atmospheric vortices is provided using the steady state model for two-cell vortices of Vatistas (1998). These include the high Rossby number dust devils, tornadoes, and waterspouts. In addition the two-cell wing tip vortex of Snedeker (1972) will be included.

On May 1999, a catastrophic tornado occurred near Mulhall, Oklahoma. The damage inflicted structures corresponded to an F4-level tornado and resulted in the deaths of several people. A Doppler on Wheels (DOW) mobile radar near Mulhall recorded this tornado and documented a multiple vortex structure. In the Fig. 3.1.1 the measured pressure profile for the Mulhall tornado (Lee and Wurman, 2005) is compared with the theoretical model of Vatistas (1998). It is clear that the theoretical model correlates well the observations.

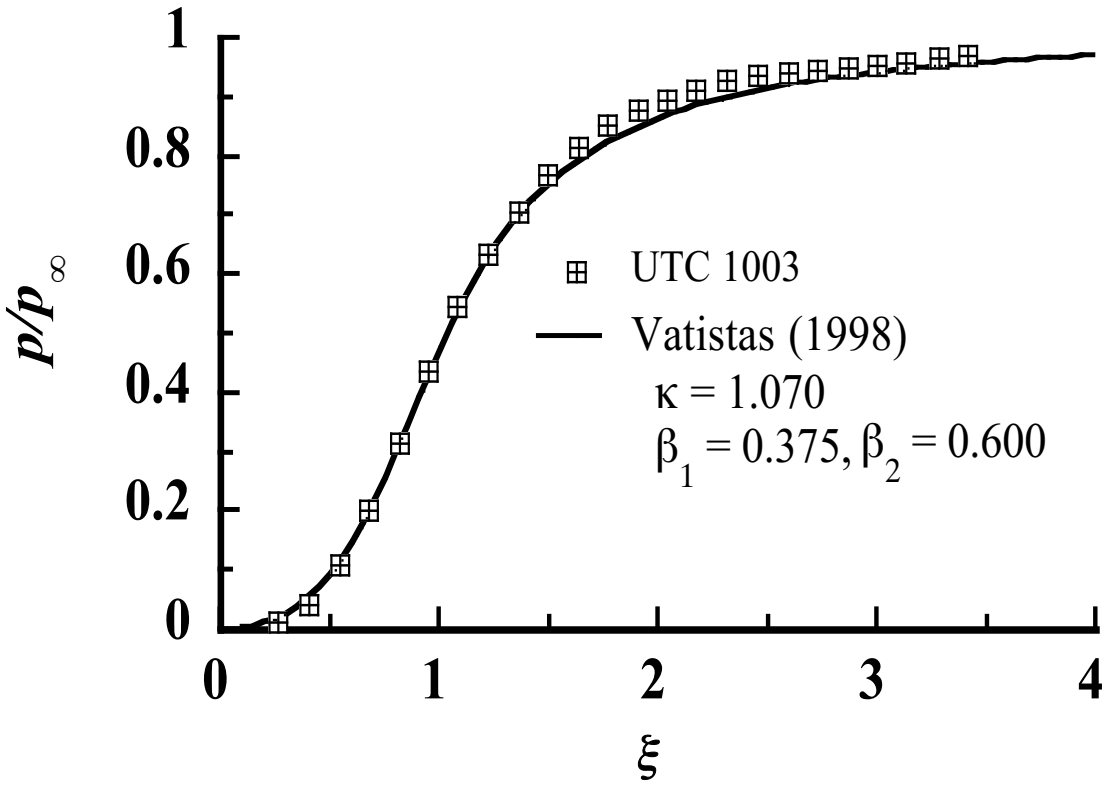

Figure 3.1.1. Comparison of the static pressure with the present two-cell incompressible vortex model and the experimental data of the Mulhall Tornado on 3 May 1999. (Discretized data from Lee and Wurman (2005))

Often tornadoes are also investigated under laboratory conditions using vortex simulators. Zhang and Sarkar (2008) studied the effects of simulated tornadoes using 2-D Particle Image Velocimetry (PIV) technique. In Fig. 3.1.2., a comparison between the model and the observations given by Zhang and Sarkar. Once more the model shows a fair agreement with the experimental velocity profile.

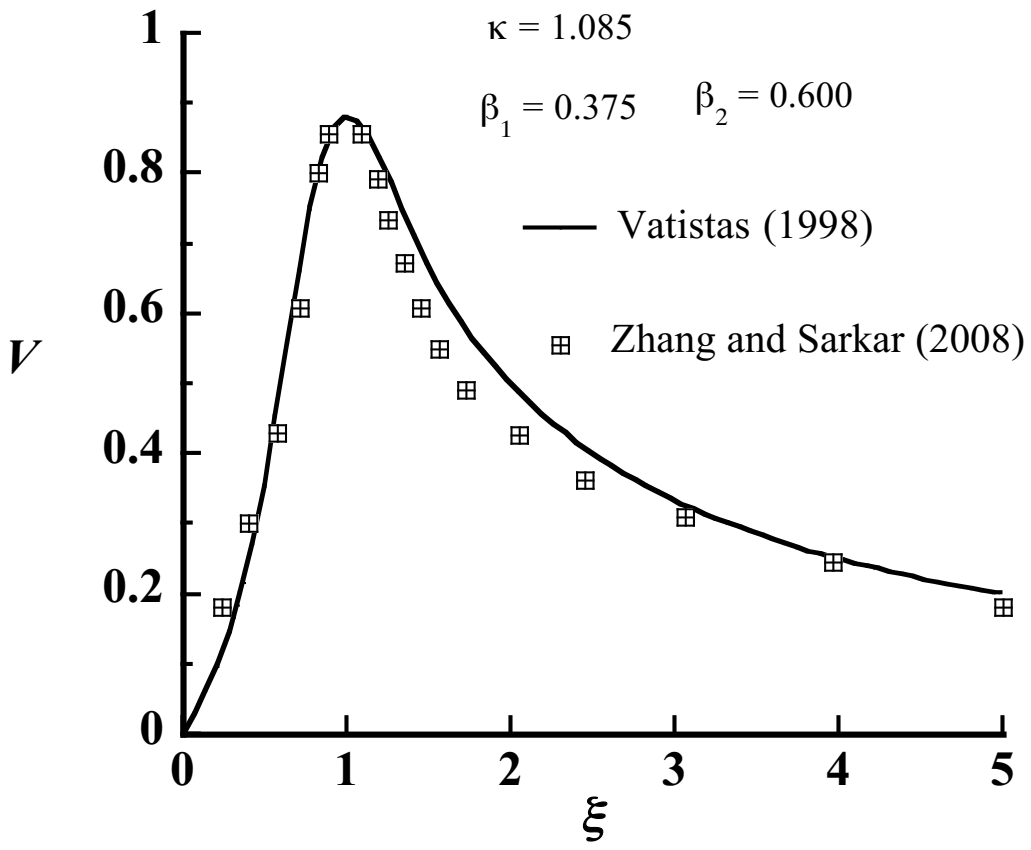

Figure 3.1.2. Comparison of the tangential velocity component with the present two-cell incompressible vortex model and the experimental data of the laboratory-simulated tornado. (Discretized data from Zhang and Sarkar (2008)).

Most dust devils appear as circular rings forming small-scale vertical vortices and can be either one- or two-celled. The observed tangential velocity plot for a double-cell dust devil, collected in northwest Texas (Blustein et al., 2004) is presented and correlated with the theoretical model under consideration in Fig. 3.1.3.

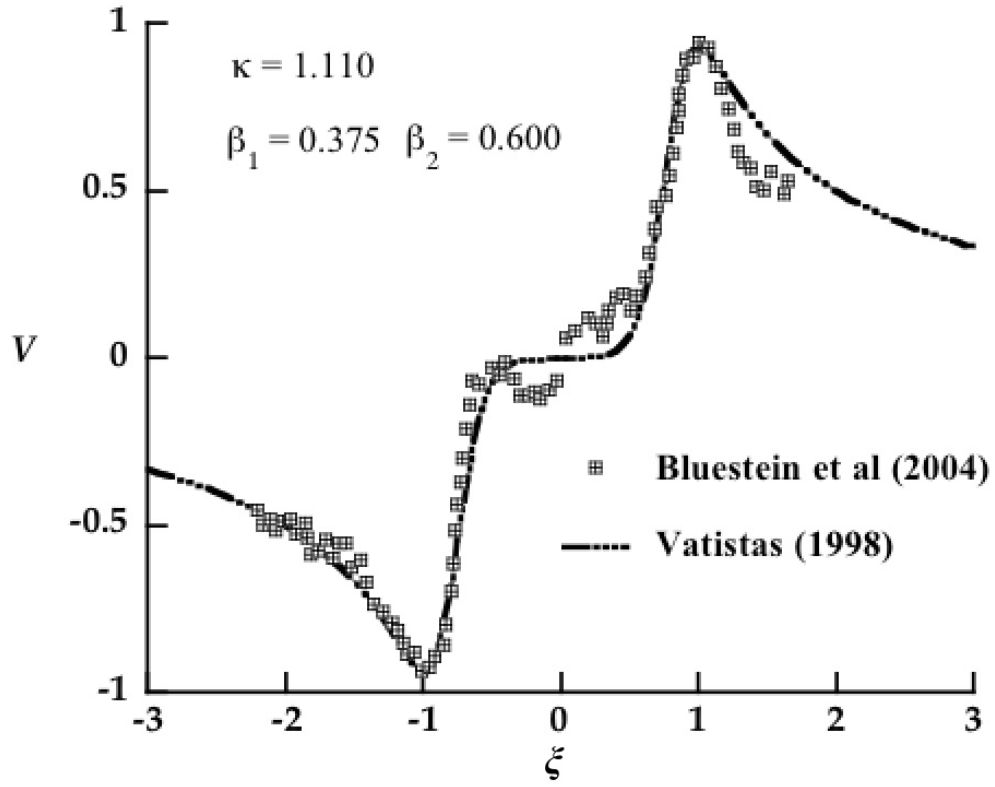

Figure 3.1.3. Comparison of the tangential velocity component with the present two-cell incompressible vortex model and the experimental data of the Texas dust devil on 25 May 1999. (Discretized data from Bluestain et al. (2004))

The aerodynamics of mechanical vortices is another important field where two-cell vortices may appear. In the early 1970s attention was placed on reducing the hazard caused by the aircraft tip vortices by altering the wake at the point of inception. Snedeker (1972) performed experiments with the aim to explain why wing tip vortices weaken under the presence of an axial jet. His results showed that an originally single-cell vortex could transform into to two-cell by introducing an axial jet very close to the starting point of the vortex. Snedeker's experimental tangential velocity profile of a tip vortex under the influence of an axial jet, along with the theoretical is shown in Fig. 3.1.4.

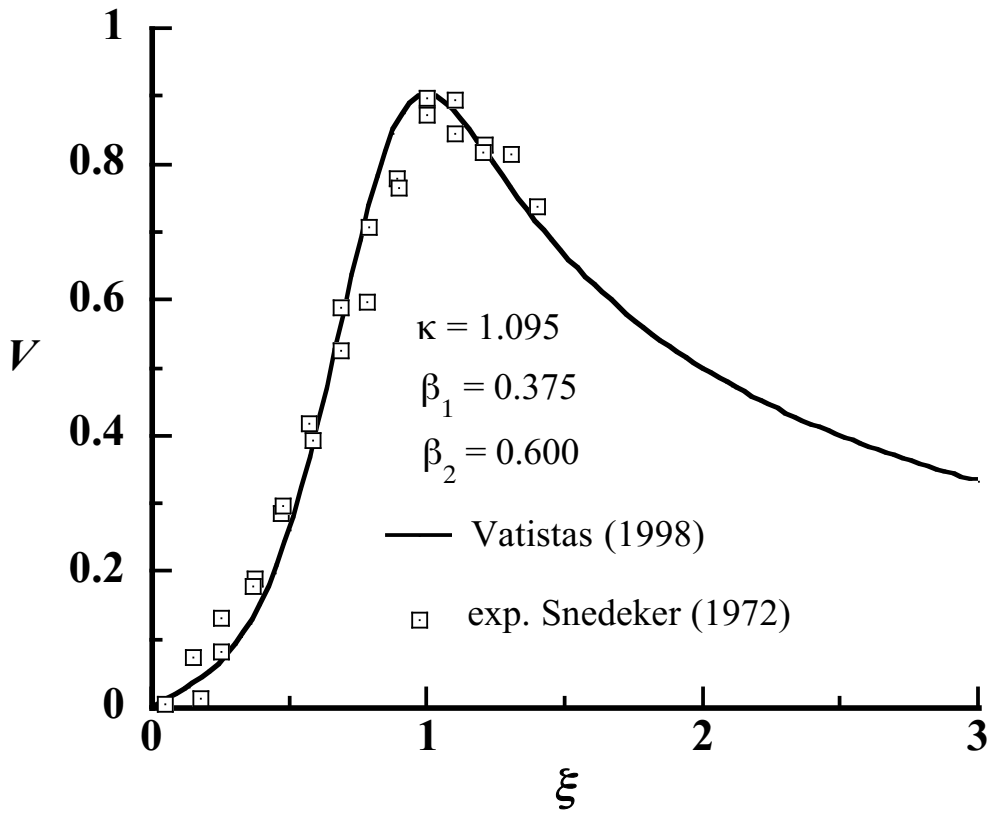

Figure 3.1.4. Comparison of the tangential velocity component with the present two-cell incompressible vortex model and the experimental data of aerodynamic vortices. (Discretized data from Snedeker (1972))

Having illustrated the ability of the Vatistas (1998) model to correlate double-cell, steady vortices, we now proceed to discuss the results of the present extension of the theory that includes the temporal effects (decaying).

3.2 Time Decay of Two-Cell Vortices

It has been shown in the subsection 2.2.1 that via proper variable transformations, a steady vortex can be converted into a time decaying. Initially, $\tau = 0$, the vortex is at its steady state condition. At $\tau = 0^+$ and under the influence of viscous effects, the vortex will start to decay with time. The velocity components of a decaying two-celled vortex for different time levels, obtained solving Eqs. (2.2.18), (2.2.19), and (2.2.20), are shown in Fig. 3.2.1 (a)-(b)-(c). It is clear that all velocity components decrease with τ, approaching zero as $\tau \to \infty$.

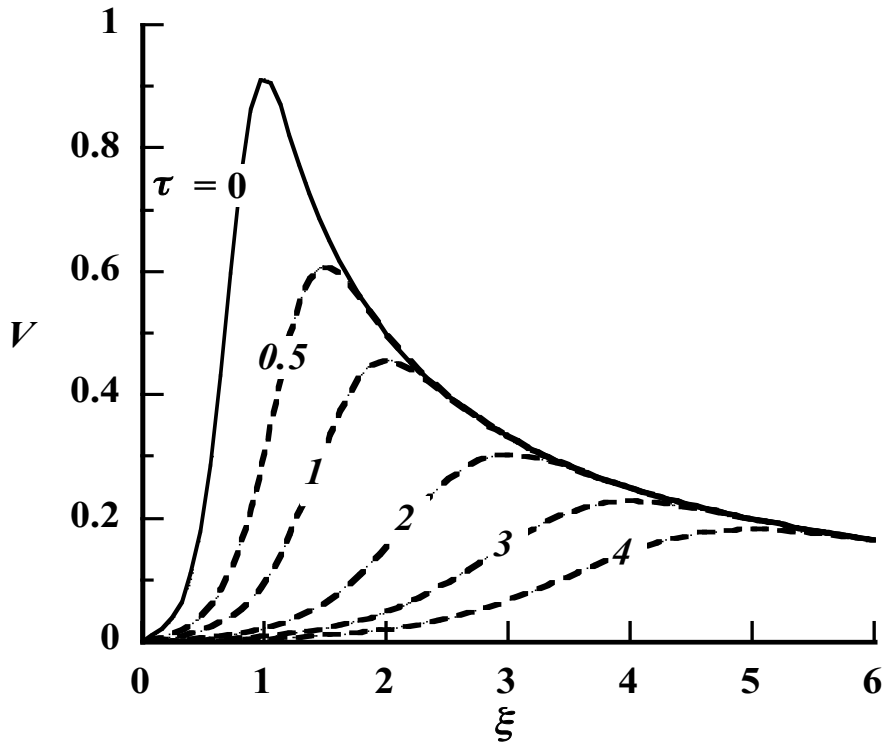
1
0.8
0.6
0.4
0.2
0
V
τ = 0
0.5
1
2
3
4
0
1
2
3
4
5
6
ξ

(a)

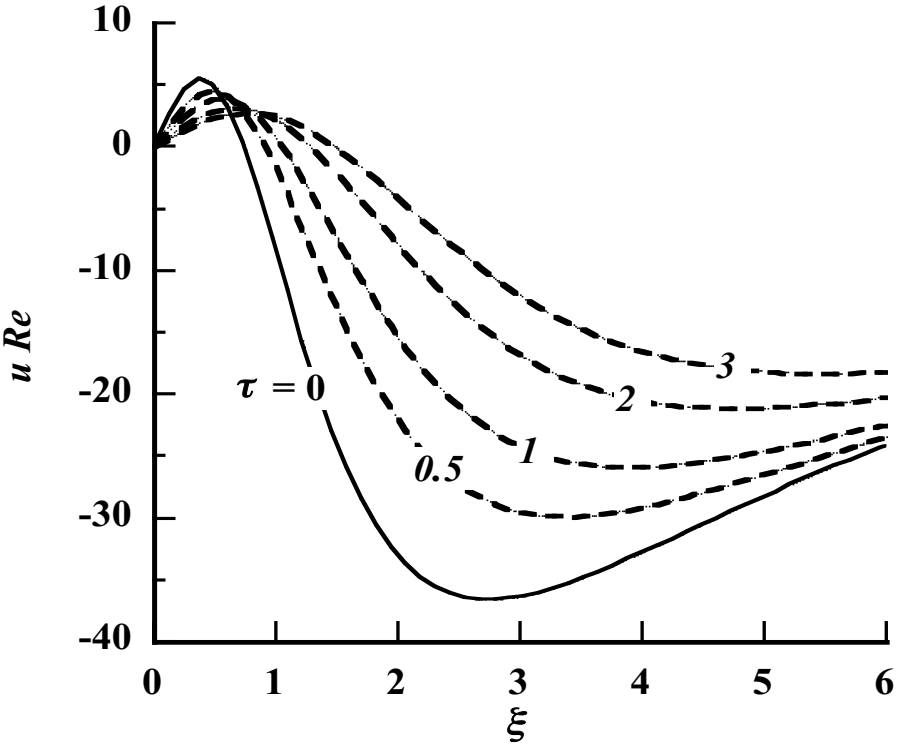
10
0
-10
-20
-30
-40
u Re
τ = 0
0.5
1
2
3
0
1
2
3
4
5
6
ξ

(b)

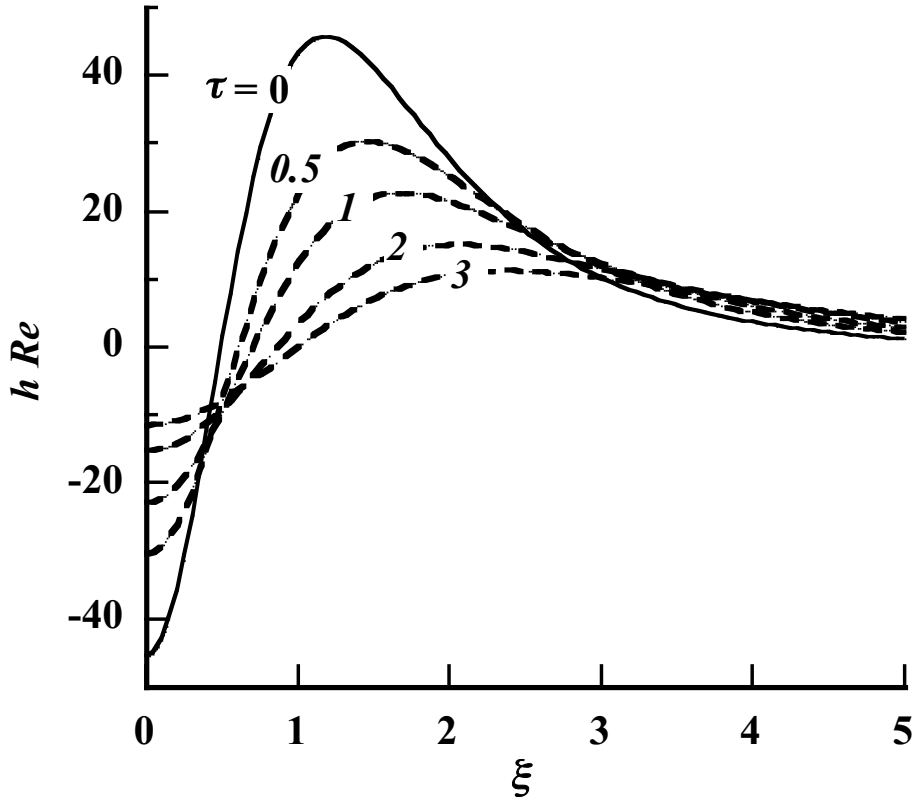

(c)

Figure 3.2.1. Temporal distribution of velocity components during the decaying of two-celled vortices (a) tangential velocity, (b) radial velocity, and (c) axial velocity ($\kappa = 1.1$, $\beta_1 = 0.375$, $\beta_2 = 0.6$).

Taking the partial derivative of the tangential velocity (Eq. 2.2.18) with respect to the radius, and setting it equal to zero we obtain the radius where the tangential velocity attains its maximum value at any τ.

In Fig. 3.3.2, the results of the present two-cell vortex are compared with the corresponding to one-cell Lamb (1932)-Oseen (1912) (or Burgers (1948)) vortex. The

last figure shows that the temporal core radius grows linearly and much faster with time than the Lamb-Oseen one-cell vortex where the core is proportional to $\tau^{1/2}$.

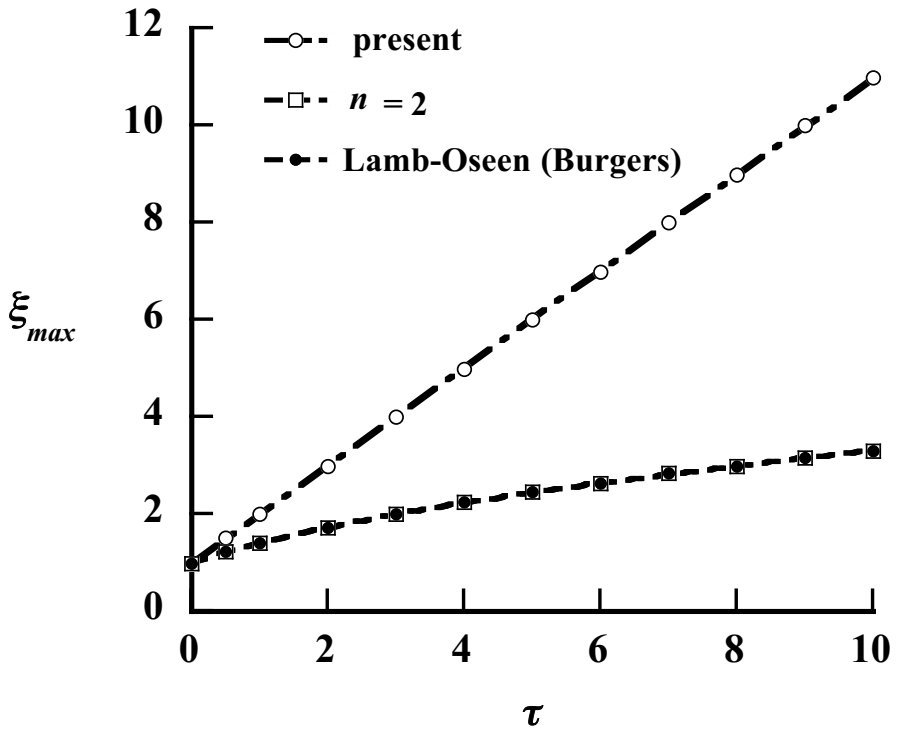

Figure 3.2.2. Distribution of maximum values for radius versus time

If we now substitute the values for maximum radius into the equation for tangential velocity (Eq. 2.2.18), we obtain the maximum tangential component versus time.

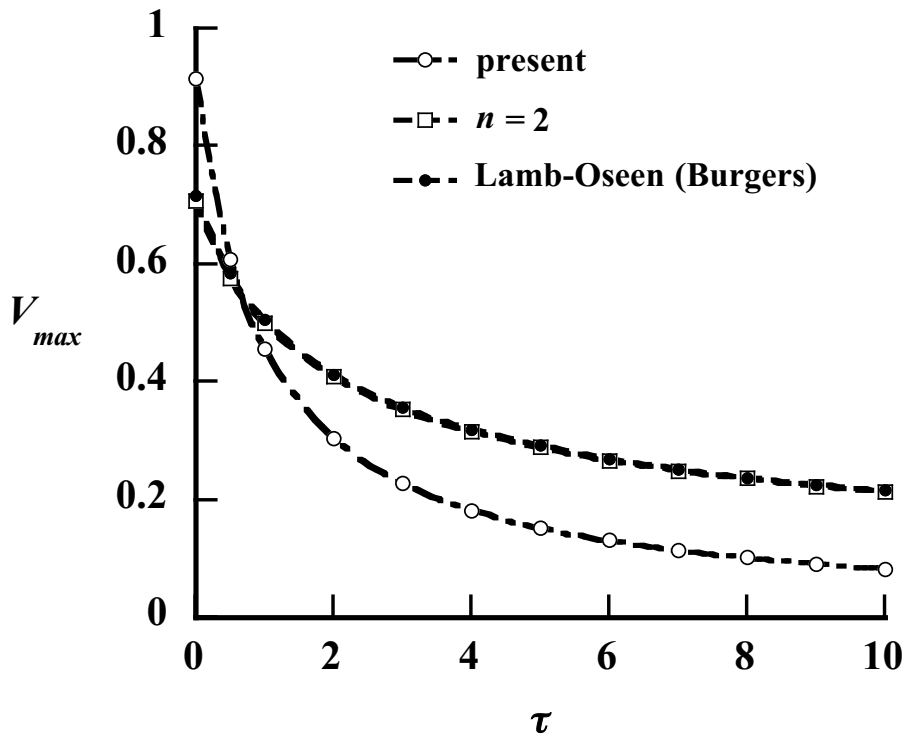

Figure 3.2.3. Distribution of maximum values for tangential velocity versus time

In Fig. 3.2.3, the present model is compared with the Lamb (1932)-Oseen (1912) vortex models, where it is seen that the maximum value of the tangential velocity declines considerably faster in two-cell vortex than in a single. The cause of this behavior may be attributed to the added friction due the concavity developed in the tangential velocity profile inside the core Fig. 3.2.4. This could also explain the observed reduction in the maximum velocity and increase of the core radius in Snedeker's experiments, when the vortex was transformed into two-celled by the introduction of an axial jet. Previously it was argued that the fast decay was due to the added turbulence caused by the introduction of the central jet. Our calculations base on the recent work of Vatistas et al. (2015) however, show that the effective vortex

Reynolds number is low for the vortex to be turbulent enough that will explain the rapid decay.

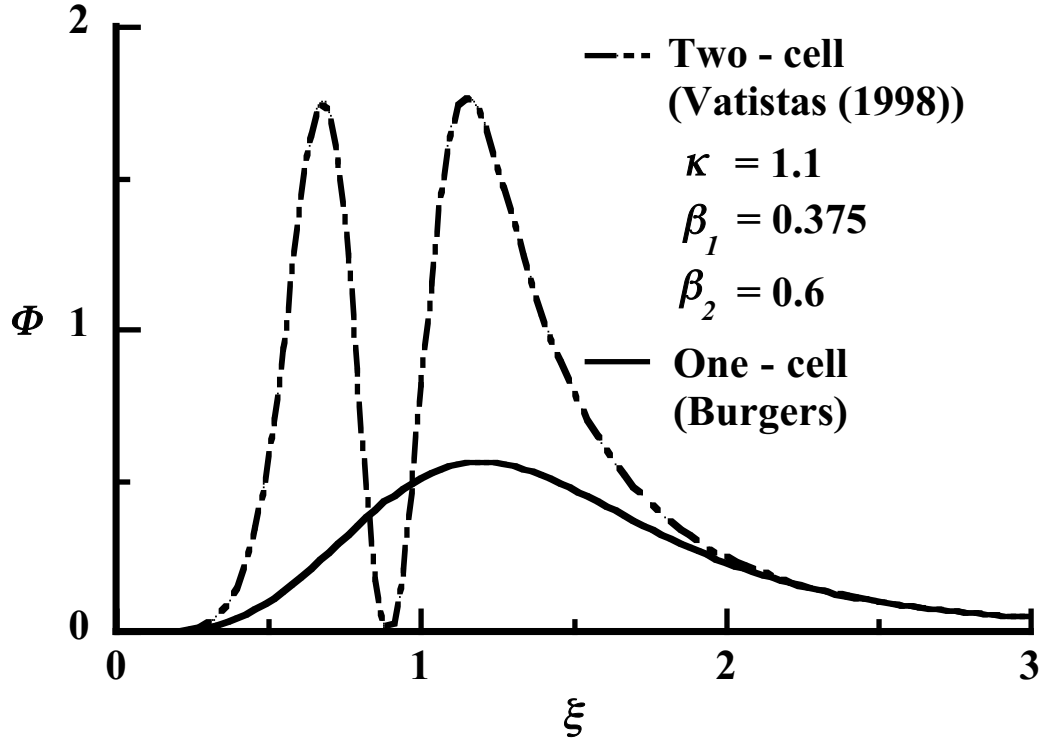

Figure 3.2.4. Distribution of the dissipation function for steady two - and one - cell Vortices

3.3 The Steady-State Two-Cell Compressible Version of the Vortex Model

In this chapter the results of the analysis for two-cell compressible vortices are presented. All the calculations were made taking the Mach number equal to 0.6 and a Prandtl number equal to 2/3. An examination, *vis-à-vis* the influence of Pr (around 0.70) revealed insignificant differences in the temperature profile. Thus, in all the subsequent calculations Pr = 2/3, where an exact solution for the energy equation for one-cell vortex is known (Vatistas and Aboelkassem (2006)) was utilized for all computations. Furthermore, the scaling parameters are set as follows: κ =1.1, β_1= 0.375 and β_2= 0.6. The value of λ is obtained solving Eq. (2.2.10) numerically.

The three velocity components (radial, axial and tangential) are calculated from Eqs. (2.2.8), (2.2.7), (2.2.9) respectively and the corresponding graphs are depicted in Figs. 3.3.1, 3.3.2 and 3.3.3. Additionally, the evaluation of density, static pressure and temperature are determined using the Matlab platform. More precisely, the rule of 1/3 composite Simpson applying the "quadl" command was employed to solve the equations. The error is estimated to be 10^{-6}.

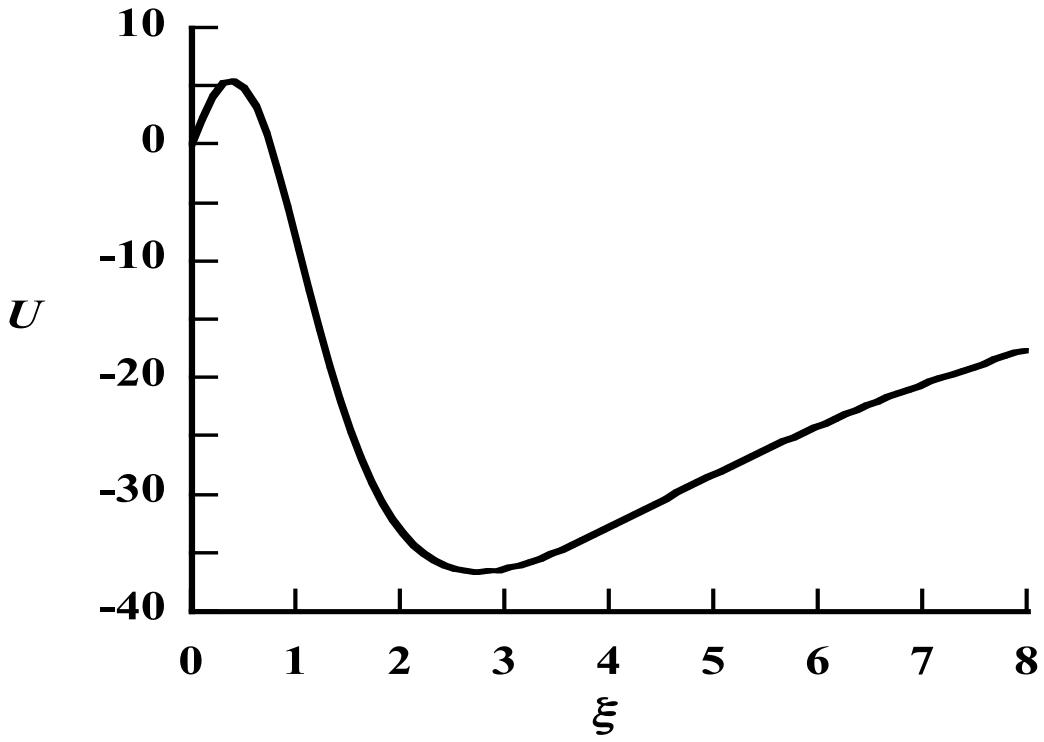

Figure 3.3.1. Variation of the dimensionless radial velocity vs. radius for $M_o = 0.6$, $\kappa = 1.1$, $\beta_1 = 0.375$, and $\beta_2 = 0.6$.

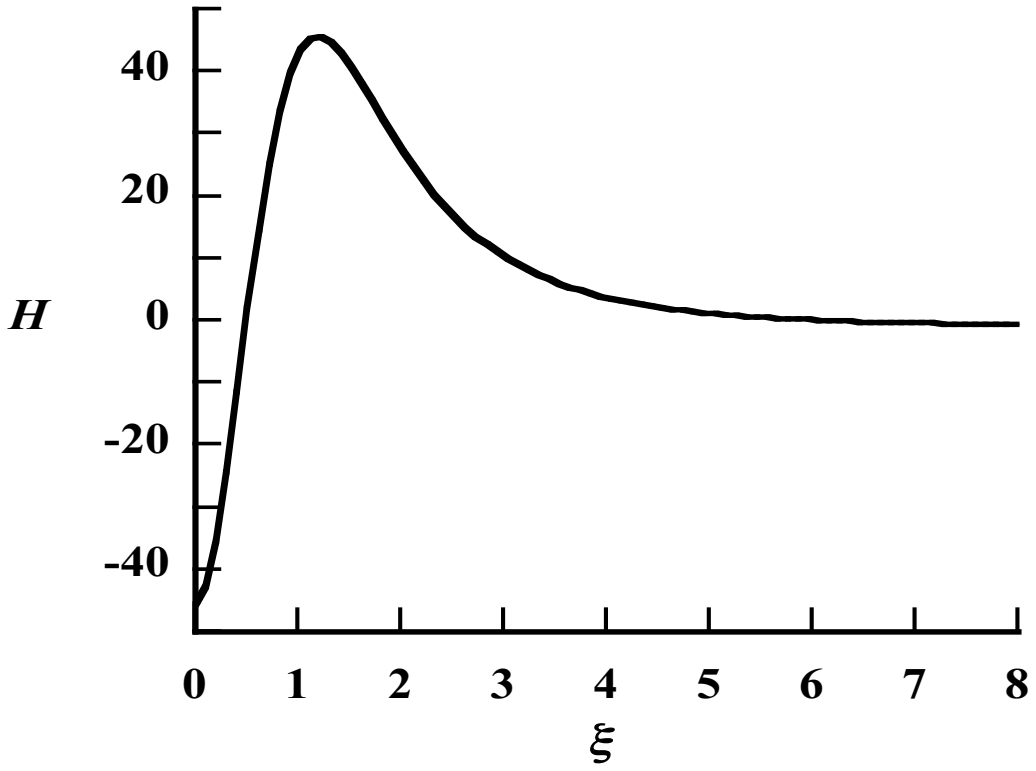

Figure 3.3.2. Variation of dimensionless axial velocity vs. radius for M_o=0.6, $\kappa = 1.1$, β_1=0.375, and β_2=0.6.

The radial velocity component is shown in Fig. 3.3.1. It is clear that most of the fluid travels from the outer periphery towards the center of the vortex. A small portion of the flow near the center diverges. In order to satisfy continuity, the axial velocity component develops the wake-like profile shown in Fig. 3.3.2. It has been verified that the values of the axial and radial velocity components do satisfy continuity.

In all previously mentioned theories (except Rankine's (1858)), the steady vortex is preserved by transfering vorticity from far towards the center by the radial velocity in order to replenish the vorticity that has been difussed outwards.

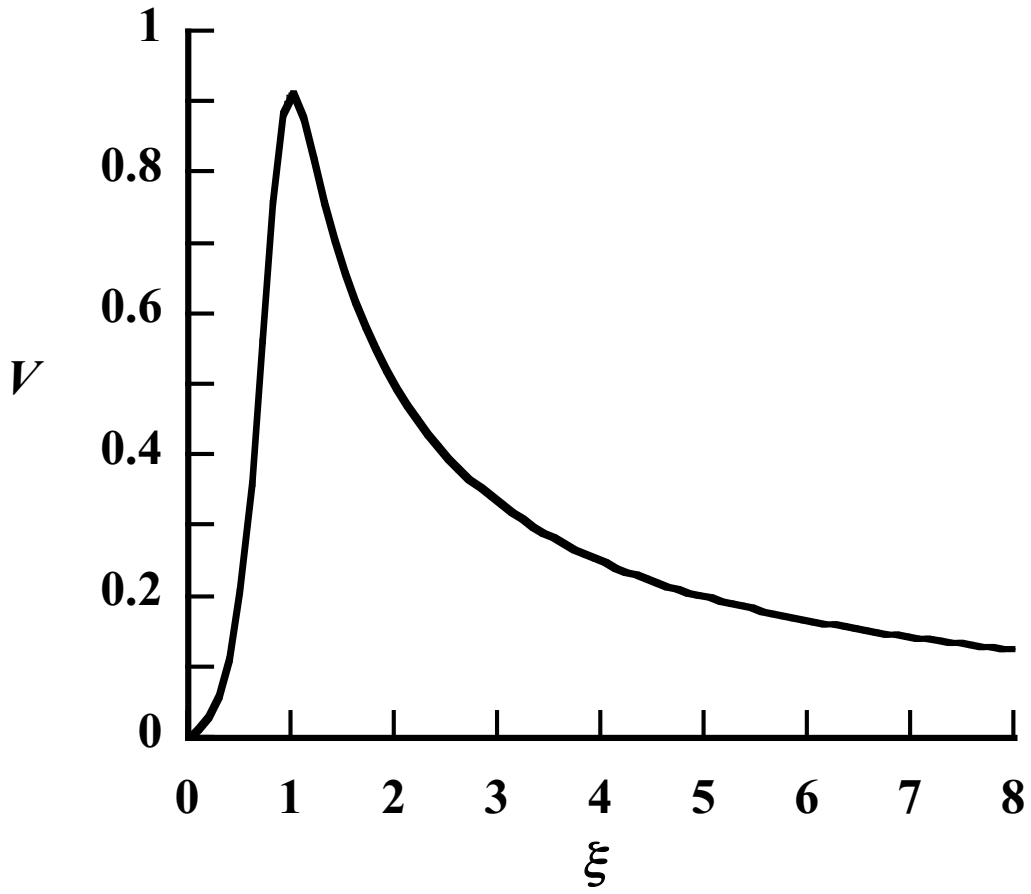

Figure 3.3.3. Variation of dimensionless tangential velocity vs. radius for M_o=0.6, $\kappa = 1.1$, β_1=0.375, and β_2=0.6.

Outside the vortex core the tangential velocity profile shown in Fig. 3.3.3, exhibits the classical free-vortex like characteristic by increasing hyperbolically, as the fluid travels towards the center, reaching a maximum value at $\xi = 1$. For smaller radii (inside the core), the tangential velocity declines, but it does not follow the

forced-like vortex mode, a characteristic of one-cell vortices. For values of ξ in [0, 1] the tangential velocity profile bends away from the linear form. This feature could be attributed to the positive radial local flow that is taking place in the inner cell.

Explanation of Temperature Behavior

The behavior of temperature distribution (see Fig. 3.3.7.) can be explained with the help of radial rate of change temperature equation. The cause for the temperature development can be identified using the following equation,

$$\frac{d\Theta}{d\xi} = -\Pr(\gamma-1)M^2{}_o\left[\frac{\left(1+\beta_2\xi^2\right)^{\frac{Pr\kappa}{2\beta_2}}}{\left(1+\beta_1\xi^2\right)^{\frac{Pr}{2\beta_1}}}\right]^{\lambda}\frac{1}{\xi}\int_0^{\xi}\left[\frac{\left(1+\beta_1\xi^2\right)^{\frac{Pr}{2\beta_1}}}{\left(1+\beta_2\xi^2\right)^{\frac{Pr\kappa}{2\beta_2}}}\right]^{\lambda}\left(UV^2+f\xi\right)d\xi \rightarrow$$

$$-\frac{d\Theta}{d\xi} = \Pr(\gamma-1)M^2{}_o\left[\frac{\left(1+\beta_2\xi^2\right)^{\frac{Pr\kappa}{2\beta_2}}}{\left(1+\beta_1\xi^2\right)^{\frac{Pr}{2\beta_1}}}\right]^{\lambda}\frac{1}{\xi}\int_0^{\xi}\left[\frac{\left(1+\beta_1\xi^2\right)^{\frac{Pr}{2\beta_1}}}{\left(1+\beta_2\xi^2\right)^{\frac{Pr\kappa}{2\beta_2}}}\right]^{\lambda}UV^2d\xi + \Pr(\gamma-1)M^2{}_c\left[\frac{\left(1+\beta_2\xi^2\right)^{\frac{Pr\kappa}{2\beta_2}}}{\left(1+\beta_1\xi^2\right)^{\frac{Pr}{2\beta_1}}}\right]^{\lambda}\frac{1}{\xi}\int_0^{\xi}\left[\frac{\left(1+\beta_1\xi^2\right)^{\frac{Pr}{2\beta_1}}}{\left(1+\beta_2\xi^2\right)^{\frac{Pr\kappa}{2\beta_2}}}\right]^{\lambda}f\xi d\xi$$

Cooling of fluid element due to expansion (C)

Heating of fluid element due to dissipation (F)

(3.3.1)

The negative sign in front of the derivative indicates that the fluid is moving from the outer periphery towards the vortex center.

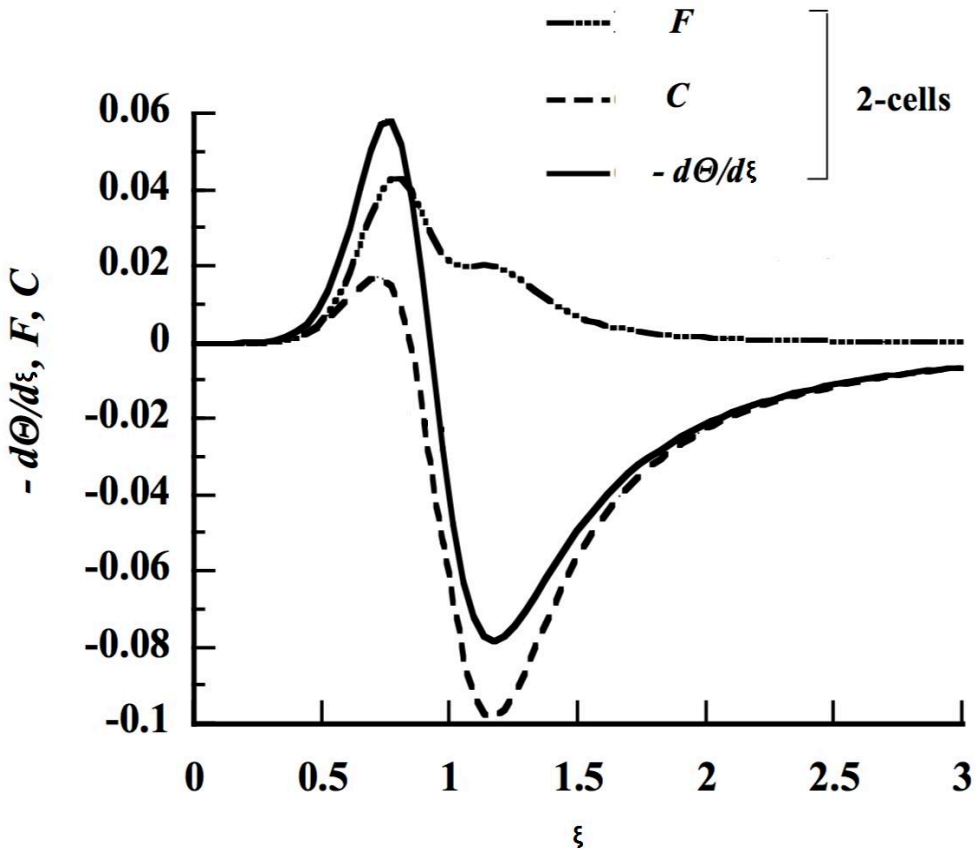

Figure 3.3.4. Net effect of heating and cooling of fluid element due to viscous dissipation and fluid expansion respectively in a laminar compressible 2-cell vortex for M_o =0.6, Pr =2/3, $\kappa = 1.1$, $\beta_1 = 0.375$, and $\beta_2 = 0.6$.

As shown in Figure 3.3.4, the development of the temperature is the outcome of competition between cooling (*C*) due to infinitesimal fluid element expansion and heating up (*F*) due to dissipation. The net effect of *F* and *C* will decide whether the temperature increases or decreases.

For the better understanding of temperature change, the expressions for the density and the pressure are also solved using the numerical values for temperature (Eq. (2.3.31). The equations of Vatistas (2006) were used respectively in order to calculate the values of the density and the pressure.

$$\beta = \frac{exp\left[\gamma M_o^2 \left\{\int_0^{\xi} \frac{V^2}{\xi\Theta} d\xi\right\} - \int_0^{\infty} \frac{V^2}{\xi\Theta} d\xi\right]}{\Theta} \qquad (3.3.2)$$

$$\Pi = \frac{exp\left[\gamma M_o^2 \left\{\int_0^{\xi} \frac{V^2}{\xi\Theta} d\xi\right\} - \int_0^{\infty} \frac{V^2}{\xi\Theta} d\xi\right]}{\gamma M_o^2} \qquad (3.3.3)$$

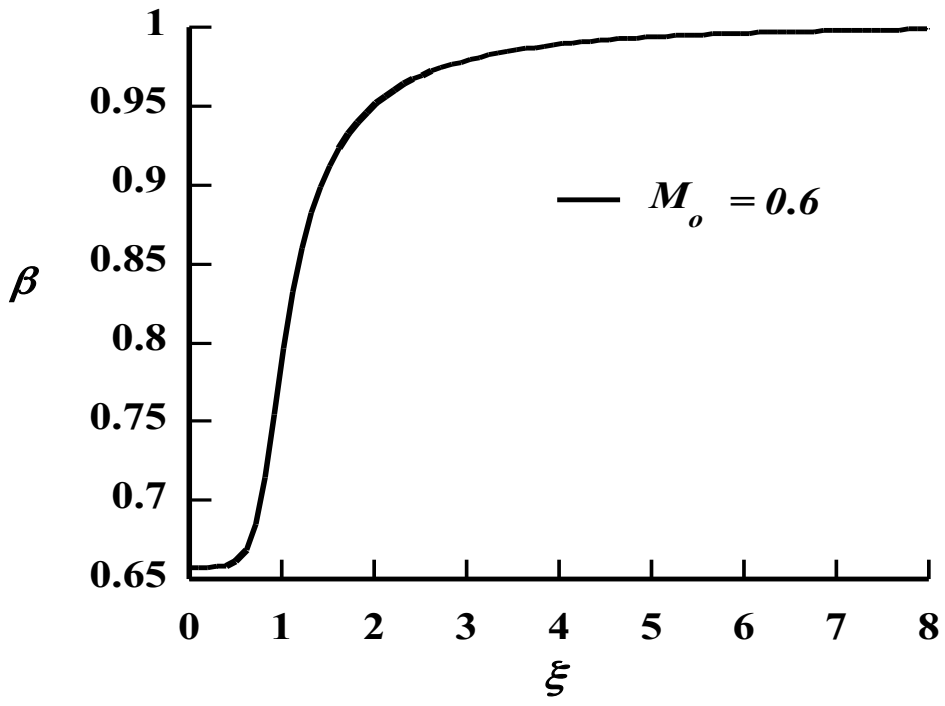

Figure 3.3.5. Radial distribution of density (β) for M_o=0.6, Pr =2/3, κ = 1.1, β_1= 0.375, and β_2=0.6.

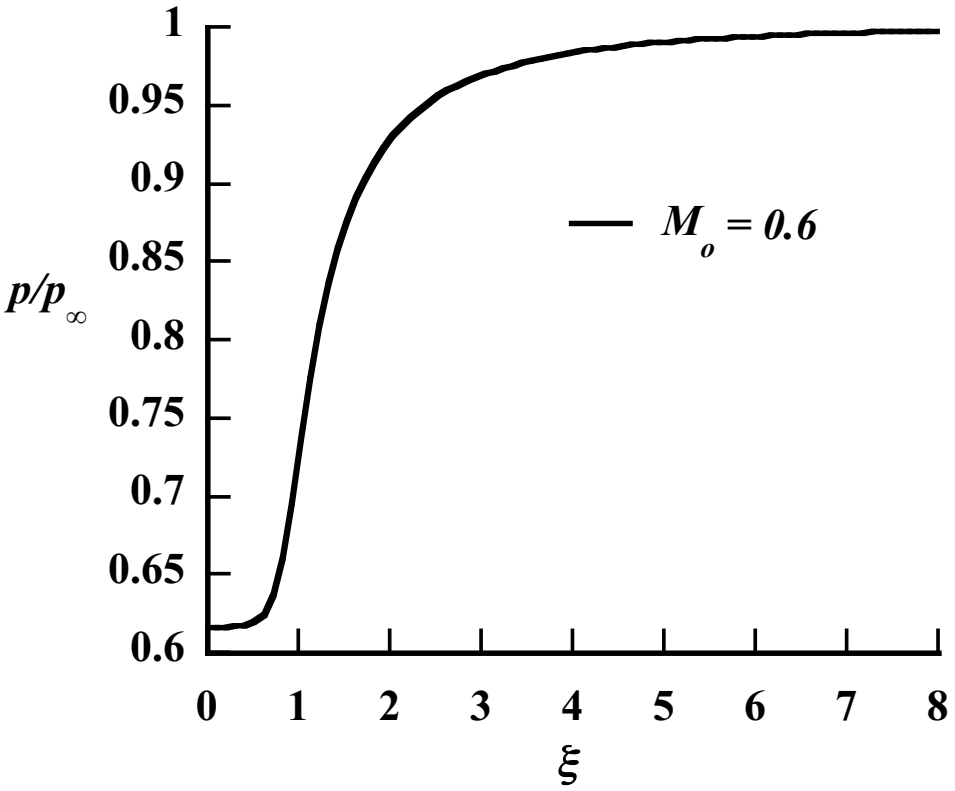

Figure 3.3.6. The plot of dimensionless pressure (Π) along the radial direction for M_o = 0.6, Pr =2/3, κ = 1.1, β_1 = 0.375, and β_2 = 0.6.

According to Fig. 3.3.4., as the fluid moves towards the vortex center, two elementary events are taking place:

- Mechanical dissipation (*F*), where the change in temperature is always positive.
- The cooling effect (*C*), where the change in temperature is negative due to the expansion of fluid element ($1 \le \xi \le \xi_\infty$) and positive after due to its contraction ($0 \le \xi \le 1$).

Initially, as the fluid element is moving in the stream-wise direction (negative radial velocity), the pressure decreases, see Fig. 3.3.6. Since the amount of matter inside the fluid element is fixed, when its volume increases (pressure reduces) the density of the fluid element must decrease (see Figure 3.3.5). Therefore, its temperature decreases due to element dilation (C) and rises due to dissipation (F). However, in $\sim 1 \leq \xi < \xi_\infty$ Fig. 3.3.4 shows that $F + C$ is negative and therefore the temperature will drop. In the interval $\sim 0.2 \leq \xi \leq \sim 1$ $F + C$ is positive (pressure and density increase), and thus the temperature will also increase. The temperature will not change in $0 \leq \xi \leq \sim 0.2$ because $F = C = 0$. Consequently, in this interval both the pressure and density will remain also constant.

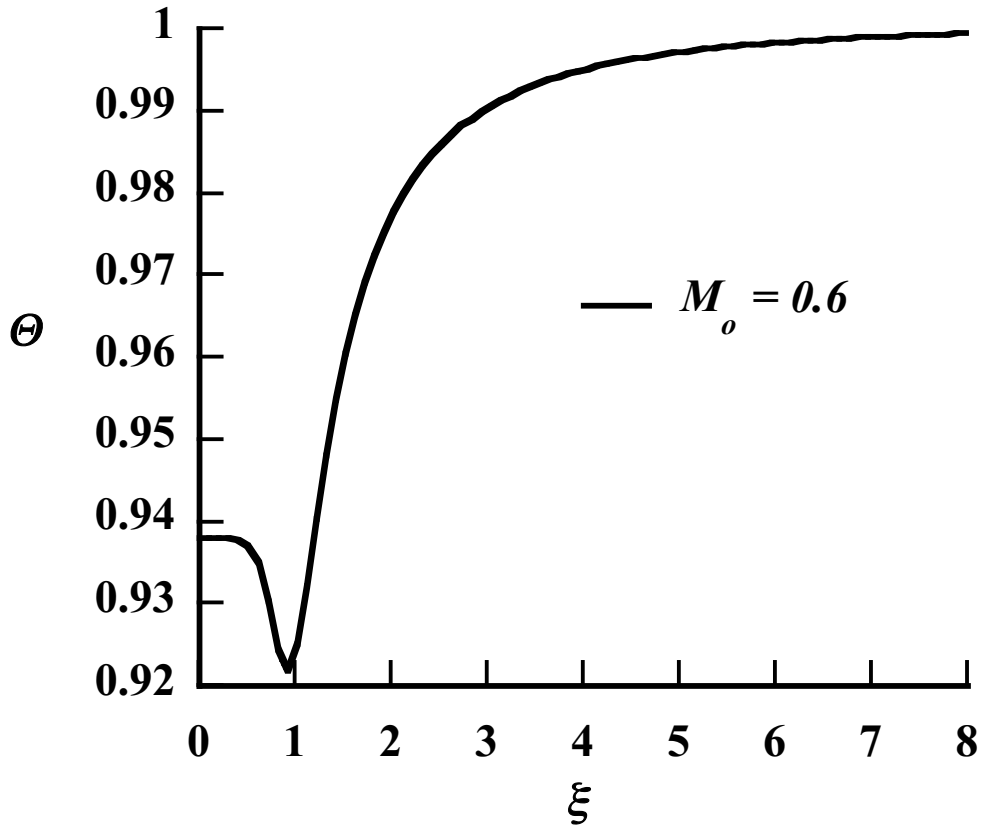

Figure 3.3.7. Radial distribution of temperature (Θ) for $M_o = 0.6$, $\kappa = 1.1$, $\beta_1 = 0.375$, and $\beta_2 = 0.6$.

The temperature distribution is presented in Fig. 3.3.7. It is apparent that its value declines gradually with decreasing ξ, or as the fluid element travels from the outer periphery towards the center, reaching a minimum temperature close to $\xi = 1$ and then it rises, attaining a small plateau in the neighborhood of the center. The identification of the cause of the last effect will be attempted next. The reason of the last effect is due to the fact that cooling because of fluid element expansion, is larger in magnitude than the heating up due to mechanical dissipation see Fig. 3.3.4. As the infinitesimal element moves towards a region of lower pressure it dilates. Since the

amount of matter inside the fluid element is fixed, when its volume increases the density inside the fluid element must decrease (see Figure 3.3.5). Since both the temperature and density drops the pressure ought from the state equation to also decrease, Fig. 3.3.6.

For values of radii $0 \leq \xi \leq 1$ (inside the core), the cooling is less than dissipation and thus the temperature rises. In this interval the density decreases faster than the increase of temperature causing the pressure to decrease further. Inside the interval $0 \leq \xi \leq 1$ all properties attain a plateau thus they remain constant.

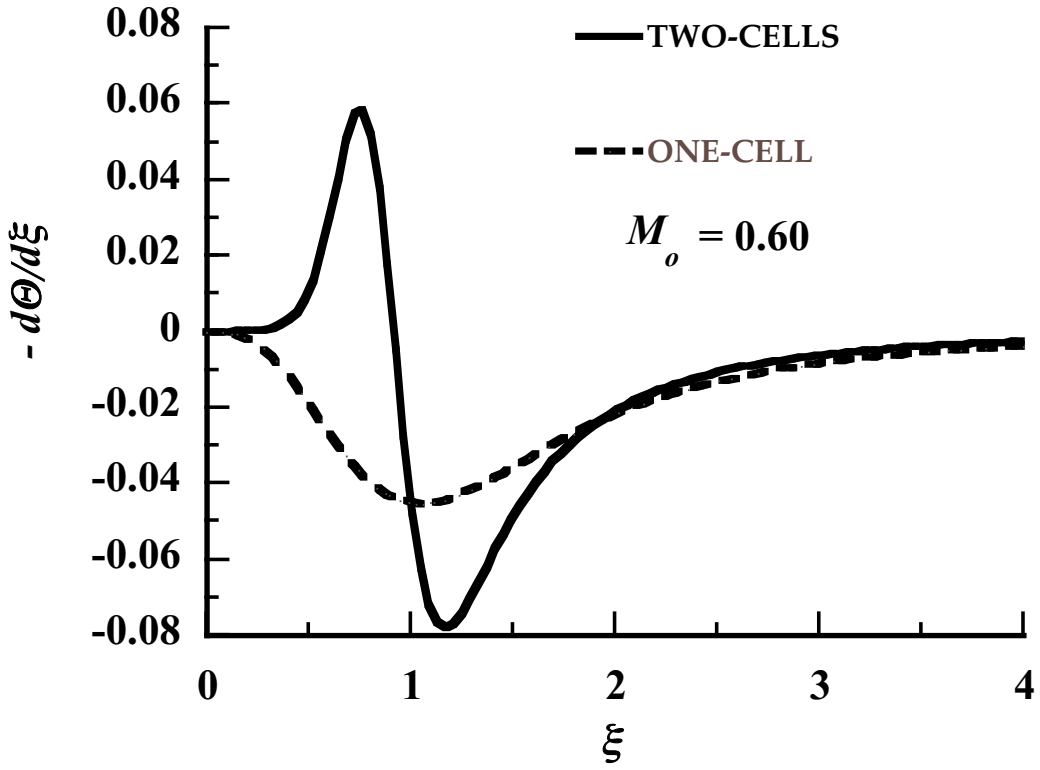

Figure 3.3.8. Comparison of net effect of heating and cooling of fluid element due to viscous dissipation and fluid expansion respectively in a laminar compressible one- and 2-cell vortex for M_o=0.6, Pr =2/3, κ=1.1, β_1=0.375, and β_2=0.6.

In Fig. 3.3.8., a comparison of net effect of fluid element for the case of one- and two-cell vortex is illustrated. According to the graph, in $1.5 < \xi < \xi_\infty$, a similar pattern of net effect is noticed in both cases. The temperature decreases gradually as the cooling effect (*C*) is greater than the dissipation (*F*) for these values of radii. However, in $1.5 < \xi < 0$, where the fluid element is in the core area, several differences are illustrated. Specifically, in the case of two-cells, two temperature peaks are noticed (one minimum and one maximum peak for radii $0 \le \xi \le 1$), while in

the case of one-cell only one minimum peak is obtained. This difference could be due to the reverse flow generated in the inner cell at the situation of double-cell vortex.

Therefore, the fluid element gets cold for radii $\xi = 1$ but as it moves towards the center, the temperature increases sharply due to dissipation of the reversed flow. For radius $0 \le \xi \le 0.8$, the temperature starts to decrease gradually reaching a plateau as the flow approaches the center. In the situation of one-cell vortex, only a smooth monotonic drop of temperature is observed inside the core while for radius $0 \le \xi \le 1$, the temperature rises slowly until the center.

3.3.1 Effect of Mach number on Temperature, Density and Pressure

The results of temperature for different vortex Mach numbers are plotted in Figure 3.3.9.

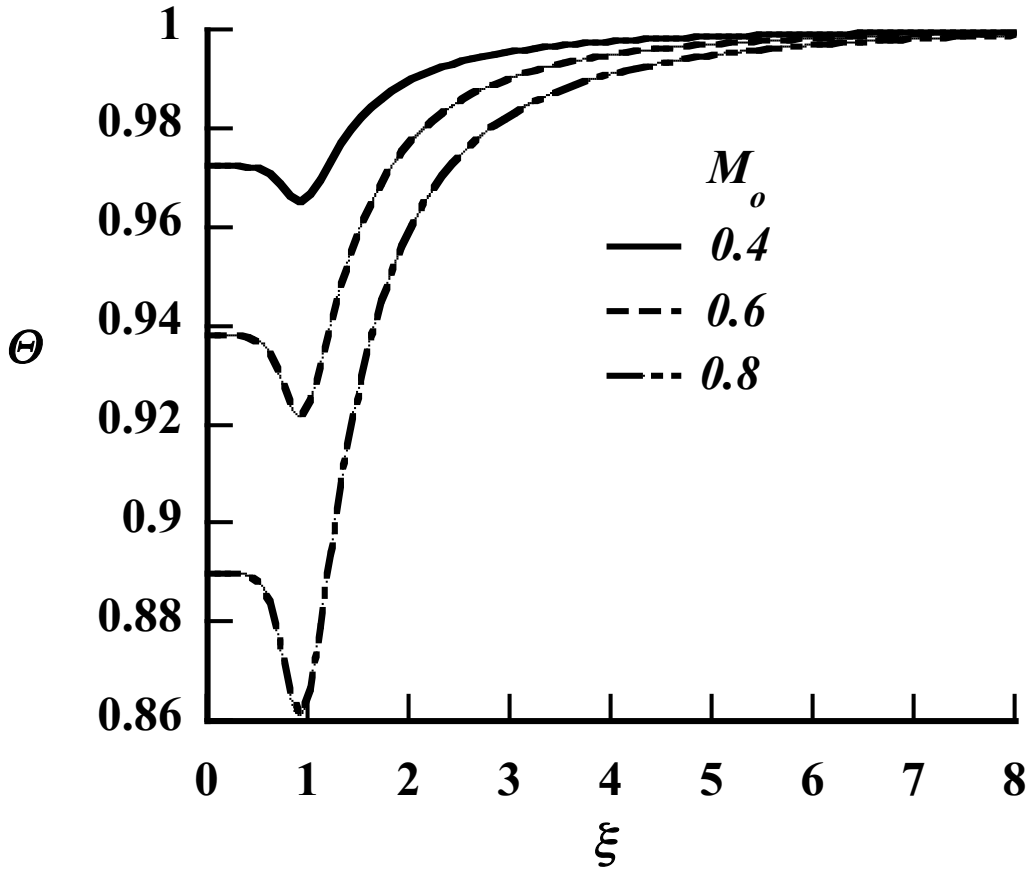

Figure 3.3.9. Radial distribution of temperature (Θ) for different Mach numbers with Pr =2/3, $\kappa = 1.1$, $\beta_1 = 0.375$, and $\beta_2 = 0.6$.

It is evident from Fig. 3.3.9. that as fluid element travels from the outer periphery to the center of the vortex; the temperature remains almost constant until

the radius ξ of 5. After that point, the temperature declines rapidly reaching the minimum temperature for radius slightly less than 1. Subsequently, it undergoes a slight increase until $\xi \sim 0.5$, and then it flattens as the fluid approaches the center of the vortex where its gradient is almost zero. It is also evident that as the Mach number increases, the coldest spot travels downwards and the temperature at the vortex center reduces. Therefore, for high values of Mach numbers, the region at vortex center is very cold compared to the periphery.

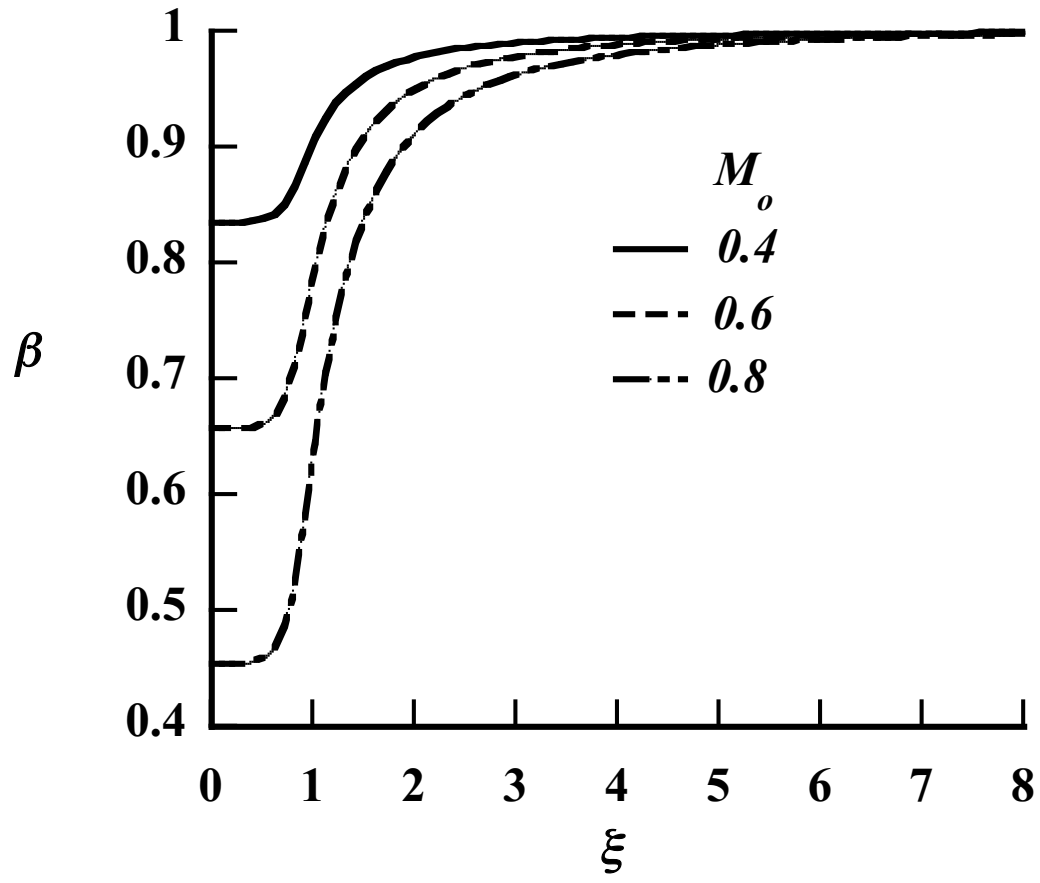

Figure 3.3.10. Radial distribution of density for different Mach numbers, with Pr=2/3, $\kappa = 1.1$, $\beta_1 = 0.375$, and $\beta_2 = 0.6$.

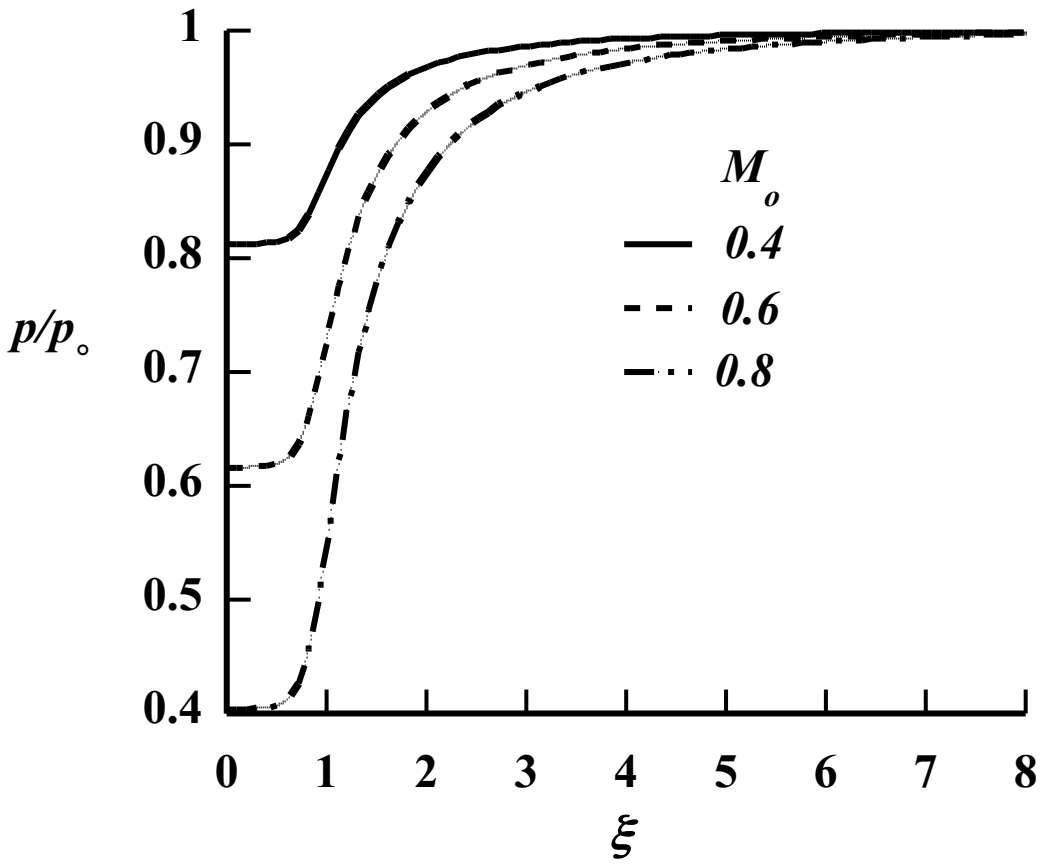

Figure 3.3.11. The plot of dimensionless pressure of (p / p_{∞}) along the radial direction for different Mach numbers, with Pr =2/3, $\kappa = 1.1$, β_1=0.375, and β_2=0.6.

Static Pressure and density are distributed in Figs. 3.3.11 & 3.3.10 respectively. Both values for pressure and density follow a similar pattern. Initially, the values start to decline monotonically as the flow moves towards the center. This drop becomes more dramatic as the flow reaches the vortex center. It is also clear that very close to the center both variables remain flat. Furthermore, as is illustrated from

the Figures, the higher the vortex Mach number is, the bigger the radial gradients become and the lower the values of pressure and density at the center of rotation are.

There are very few experiments that consider the low temperature effect in the vortex core. The experiments of Cattafesta and Settles (1992) showed clearly the presence of cooling in a vortex immersed in a supersonic stream. Also observer's testimonials regarding the tornadoes in the North Platte Valley of western Nebraska refer to the cooling effect, thinning of the ambient air, and vacuum conditions that they experienced while inside the funnel Van Tassel (1955).

Conclusions

This dissertation extended a previously derived two-cell incompressible steady state family of vortices to account for the time decay. It was also enlarged to model density variation in two-cell vortices.

Based on the conservation of mass and the Navier-Stokes equations, a new formulation was accomplished to mathematically characterize two-cell decaying vortices. The study revealed that the core vortex radius increases linearly with time while the maximum velocity reduces hyperbolically. The two-celled type was shown to decay considerably faster than the classical Lamb-Oseen. Both effects were ascribed to the hefty mechanical dissipation found in double cell vortices. It was also contended that the previously discovered vortex strength reduction in wing tip vortices with an imposed central jet is due to the changeover of the otherwise one-cell vortex into a two-cell.

The earlier *n*-family of one cell compressible vortices contribution was enlarged to account for density variation. The conservation equations of mass, momentum and energy were generalized assuming intense vortex conditions were used to model the problem. The temperature, density and pressure were then evaluated using readily available numerical integration software. It was found that along the converging flow direction, the temperature first decreased (in the outer cell), increased within the inner cell, and then was flattened in the neighborhood of the vortex center. The cause of this behavior was shown to be due to the competition of the dilation or contraction and mechanical dissipation in the fluid element. Density

and pressure near the axis of rotation, where the whirl is cold, were shown to assume sub ambient values, i.e. the gas density was dilute and the pressure was under vacuum conditions. All these thermofluid properties were found to strongly depend on the vortex Mach number.

Future Work

Although the results presented here have demonstrated the analysis of the decay of incompressible two-celled vortex and the investigation of compressible two-cell vortex approach, it could be further developed in a number of ways:

- **Extending the given work from the decay of incompressible two-cell vortex to compressible.**

  Our present vortex formulation was used to obtain the solution of the decaying incompressible two-celled vortices. A theoretical development presented by providing a space-time duality for laminar incompressible vortices. Therefore, one should formulate a new mathematical model in order to investigate the decay of compressible two-celled vortices along time. Perhaps by incorporating experimental data, we could obtain a more reliable approach.

- **Extending the given work from the compressible two-cell vortex to multi-cell vortex.**

In the present study, given a laminar two-celled vortex generated in a compressible unconfined gas, the variation of velocities distribution, temperature, density and pressure were determined. The contribution of this study can be used to explicate several problems in science. Nevertheless, in order to enhance its practical usefulness, an extended solution can be obtained by implementing the given approach to a multi-cell vortex. By allowing the model to run for a multi-

cell vortex, it could provide an enhanced approach for explaining several geophysical phenomena. This could lead to a better global optimization of tornadoes and dust devils.

References

Aboelkassem, Y., and Vatistas G. H. (2007). New Model for Compressible Vortices. Journal of Fluid Engineering, 29(8), 1073-1079.

Ardalan, K., Meiron, D. I., and Pullin, D. I. (1995, Oct.). Steady Compressible Vortex Flows: The Hollow-Core Vortex Array. Journal of Fluid Mechanics, 301, 1-17.

Bagai, A., and Leishman, G. J. (1993). Flow Visualization of Compressible Vortex Structures Using Density Gradient Technique. Experiments in Fluids, 15(6), 431-442.

Bellamy-Knights, P. G. (1980, Aug.). Viscous Compressible Heat Conducting Spiraling Flow. Quarterly Journal of Mechanics and Applied Mathematics, 33, 321-336.

Blustein, H. B., Weiss, C. C., and Pazmany, A. L. (2004). Doppler Radar Observations of Dust Devils in Texas. Mon. Wea. Rev. 132, 209-224.

Brown, S. N. (1965). The Compressible Inviscid Leading Edge Vortex. Journal of Fluid Mechanics, 22(1), 17-32.

Burgers, J. M. (1948). A Mathematical Model Illustrating the Theory of Turbulence. Advances in Applied Mechanics, 1, 171-199.

Cattafesta, L. N., and Settles, G. S. (1992). Experiments on Shock/Vortex Interaction. AIAA Paper 92-0315.

Chiocchia, G. (1989). A Hodograph Approach to the Rotational Compressible Flow of an Ideal Fluid. Quarterly of Applied Mathematics, 47, 513-528.

Colonius, T., Lele, S. K., and Moin, P. (1991, Sept.). The Free Compressible Viscous Vortex. Journal of Fluids Mechanics, 230, 45-73.

Eshita, J. I. (2014). Analysis of New Multi Cellular Vortex Model, Concordia Univerisity, Montreal

Faler, J. H., and Leibovish, S. (1977). Disturbed States of Vortex Flow and Vortex Breakdown. Physics Fluids, 20, 1385-1400.

Hall, M. G. (1966). The Structure of Concentraded Vortex Cores. Progress in Aerospace Sciences, 7(1), 53-110.

Hamel, G. (1916). Spiralformige bewegung zaher Flussigkeiten. Jahresber. Dt. Mathematiker- Vereinigung, 25, 34-60.

Han, Y. Q., Leishman, J. G., and Coyone, A. J. (1997). Measuraments of the Velocity and Turbulence Structure of a Rotor Tip Vortex. AIAA J., 35(3), 477-485.

Helmholtz, H. (1858). Uber die Integrale der Hydrodynamischen Gleichungen, Welche den Wilbelbewegungen Entsprechen, Journal für die Reine und Angewandte Mathematik, 55, 25-55.

Hollingworth, M. A., and Richards, E. J. (Nov. 1955). A Schlieren Study of the Interaction Between a Vortex and a Shockwave in a Shock Tube.

Howard, L. N., and Matthews, D. L. (1956). On the Vortices Produced in Shock Diffraction. Journal of Applied Physics, 27(3), 223-231.

Jacquin, L., and Pantano, C. (2002). On the Persistence of Trailing Vortices. Journal of Fluid Mechanics, 471, 159-168.

Kalhoran, I. M., and Smart, M. K. (2000). Aspects of Shock Wave-Induced Vortex Breakdown. Progress in Aerospace Sciences, 36(1), 63-95.

Lam, H. (1993). An Experimental Investigitation and Dimensional Analysis pf Confined Vortex Flows. (Vol. Ph.D Thesis). Montreal, Canada: Department of Mechanical Enineering, Concordia University.

Lamb, H. (1932). Hydrodynamics. Cambridge, UK: Cambridge Univ. Press.

Lee Wen-Chau, and Wurman J. (2005). Diagnased Three-Dimensional Axisymmetric Structure of the Mulhall Tornado on May 1999. J. Atmos. Sci., 62, 2373-2393.

Mack, L. (1960). The Compressible Viscous Heat-Conducting Vortex. J. Fluid Mech., 8, 284-292.

Mandella, M. J. (1987). Experimental and Analytical Studies of Compressible Vortices. (Vol. Ph.D. Thesis). Stanford, Stanford University: Dept. of Applied Physics.

Meager, A. (1961). Approximate Solution of Insentropic Swirling Flow Through a Nozzle. ARS Journal, 32, 1140-1148.

Oseen, C. W. (1912). Uber Wirbelbewegune in einer Reiben-Den Flussigkeit. Arl. Mat. Astrom. Fys., 7, 14-21.

Perez-Saborid, M., Herrada, M. A., Gomez-Barea, A., and Barrero, A. (2002, Nov.). Downstream of Unconfined Vortices: Mechanical and Thermal Aspects. Journal of Fluid Mechanics, 471, 51-70.

Prichard, W. (1970). Solitary Waves in Rotating Fluids. Journal of Fluid Mechanics, 42(1), 61-83.

Ragsdale, R. G. (1960). NASA Research on the Hydrodynamics of the Gaseous Vortex Reactor. NASA TN D-288.

Ramesh, K., Gopalarathnam, A., Granlund, K., V.Ol. M., and Edwards. J. R. (2014). Discrete-vortex method with novel shedding criterion for unsteady aerofoil flows with intermittent leading-edge vortex shedding. Journal of Fluid Mechanics, 751, 500-538.

Rankine, W. J. (1858). Manual of Applied Mechanics. London: C. Griffin Co.

Robertson, J. M. (1966). HHydrodynamics in Theory and Application. Engelwood Cliffs, Prentice-Hall Inc.

Roschke, E. J. (1966). Experimantal Investigation of a Confined, Jet-Driven Vortex Chamber. NASA CR-78550.

Rott, N. (1959). On the Viscous Core of a Line Vortex 2. Zeitschrift fur Angewandte Mathematik und Physik (1982), 10, 73-81.

Rusak, Z., and Lee, J. H. (2004, Feb.). On the Stability of a Compressible Axissymetric Rotating Flow in a Pipe. Journal of Fluid Mechanics, 501, 25-42.

Scully, M. (1975). Computation of Helicopter Rotor Wake Geometry and its Influence on Rotor Harmonic Airloads. Massachusets Institute of Technology. Aeroelastic and Structures Research Laboratory.

Sibulkin, M. (1961). Unsteady, Viscous, Circular Flow Part 1. The Line Impulse of Angular Momentum. Journal of Fluid Mechanics, 11(2), 291-308.

Sibulkin, M. (1962). Unsteady, Viscous, Circular Flow Part 3. Application to the Ranque-Hilish Vortex Tube. Journal of Fluid Mechanics, 12(2), 269-293.

Snedeker, R. S. (1972). Effect of Air Injection on the Torque Produced by a Trailing Votex. Journal of Aircraft, 9(9), 682-684.

Sullivan, R. (1959). A Two-cell Vortex Solution of the Navier-Stokes Equations. Journal of Aerospace Sciences, 26, 767-768.

Taylor, G. I. (1930). Recent work on the Flow of Compressible Fluids. Journal of the London Mathematical Society, 5, 224-240.

Van Tassel, E. L. (1955). The North Platte Valley tornado outbreak of June, 1955. Mon. Weather Rev., 83, 255-264.

Vatistas, G. H. (1998). New Model for Intense Self-Similar Vortices. Journal of Propulsion and Power, 14(4), 462-469.

Vatistas, G. H. (2004). The fundamental properties. Trans. CSME, 28, 43-58.

Vatistas, G. H., and Aboelkassem, Y. (2005, June). Time Decay of n Family of Vortices. AIIA Journal, 43(6).

Vatistas, G. H., and Aboelkassem, Y. (2006). Extension of the Incompressible n=2 Vortex into Compressible. AIAA Journal, 44(8).

Vatistas, G. H., and Aboelkassem, Y. (2006a, April). Space-Time Analogy of Self Similar Intense Vortices. AIIA Journal, 44(4).

Vatistas, G. H., Kozel, V., and Mih, C. W. (1991). A Simpler Model for Concentrated Models. Experiments in Fluids, 11, 73-76.

Vatistas, G. H., Panagiotakakos, G., and Manikis F. (2015, June). Extension of the simple Laminar n-Family of Vortices into Turbulent, Journal of Aircraft, (published online).

Von Ellenrieder, K., and Cantwell, B. J. (2000). Self-Similar Slightly Compressible Free Vortices. J. Fluid Mech., 423, 293-315.

Von Ellenriender, K., and Cantwell. B. J. (2000, Nov.). Self Similar Slightly Compressible Free Vortices. Journal of Fluid Mechanics, 423, 293-315.

Wilkins, F. M. (1964). The Role of Electrical Phenomena Associated Tornadoes. Journal of Geophysical Research, 69(12), 2435-2447.

Zhang Wei, and Sarkar Partha P. (2008). Effects of ground roughness on tordado-like vortex using PIV. Colorado: AAWE workshop, August 21-22, 2008, Vail, Colorado

Appendix A

1. Solution of the Energy Equation

$$\frac{1}{\xi}\frac{d}{d\xi}\left(\xi\frac{d\Theta}{d\xi}\right)-PrU\frac{d\Theta}{d\xi}=-Pr(\gamma-1)M^{2}{}_{c}\left(U\frac{V^{2}}{\xi}+f\right)$$

where

$$u=-\lambda\left(\frac{\xi}{1+\beta_{1}\xi^{2}}-\kappa\frac{\xi}{1+\beta_{2}\xi^{2}}\right)$$

and

$$U=\beta Reu$$

Multiply through by ξ, we take

$$\frac{d}{d\xi}\left(\xi\frac{d\Theta}{d\xi}\right)-PrU\left(\xi\frac{d\Theta}{d\xi}\right)=-Pr(\gamma-1)M^{2}{}_{c}\left(UV^{2}+f\xi\right)$$

Let,

$$J=\xi\frac{d\Theta}{d\xi}$$

Then,

$$\frac{dJ}{d\xi} - PrUJ = -Pr(\gamma - 1)M^2{}_c\left(UV^2 + f\xi\right)$$

Use the integrating actor (I) to solve the above equation.

$$I = exp\left(-Pr\int Ud\xi\right)$$

$$U = -\lambda\left(\frac{\xi}{1+\beta_1\xi^2} - \kappa\frac{\xi}{1+\beta_2\xi^2}\right)$$

$$-Pr\int Ud\xi = Pr\int\lambda\left(\frac{\xi}{1+\beta_1\xi^2} - \kappa\frac{\xi}{1+\beta_2\xi^2}\right)d\xi$$

$$\int\frac{\xi}{1+\beta_1\xi^2}d\xi = \kappa\int\frac{\xi}{1+\beta_1\xi^2}d\xi$$

Let $u = 1+\beta_1 r^2$, then $du = 2\beta_1 r dr$ or $dr = du/(2\beta_1 r)$. Hence

$$\int\frac{\xi}{1+\beta_1\xi^2}d\xi = \frac{1}{2\beta_1}\int\frac{\xi}{u}\frac{du}{\xi} = \frac{1}{2\beta_1}ln\left(1+\beta_1\xi^2\right)$$

Similarly,

$$\kappa\int\frac{\xi}{1+\beta_2\xi^2}dr=\frac{\kappa}{2\beta_2}\int\frac{\xi}{u}\frac{du}{\xi}=\frac{\kappa}{2\beta_2}ln\left(1+\beta_2\xi^2\right)$$

Then

$$-Pr\int Ud\xi=Pr\int\lambda\left(\frac{\xi}{1+\beta_1\xi^2}-\kappa\frac{\xi}{1+\beta_2\xi^2}\right)d\xi=\frac{Pr}{2\beta_1}\lambda ln\left(1+\beta_1\xi^2\right)-\frac{Pr\kappa}{2\beta_2}\lambda ln\left(1+\beta_2\xi^2\right)$$

$$=\lambda ln\left(1+\beta_1\xi^2\right)^{\frac{Pr}{2\beta_1}}-\lambda ln\left(1+\beta_2\xi^2\right)^{\frac{Pr\kappa}{2\beta_2}}=ln\left[\frac{\left(1+\beta_1\xi^2\right)^{\frac{Pr_1}{2\beta_1}}}{\left(1+\beta_2\xi^2\right)^{\frac{Pr\kappa}{2\beta_2}}}\right]^{\lambda}$$

Therefore

$$IF=exp\left(-Pr\int\lambda Ud\xi\right)=\left[\frac{\left(1+\beta_1\xi^2\right)^{\frac{Pr}{2\beta_1}}}{\left(1+\beta_2\xi^2\right)^{\frac{Pr\kappa}{2\beta_2}}}\right]^{\lambda}$$

From equation

$$\frac{dJ}{d\xi}-PrUJ=-Pr(\gamma-1)M^2{}_o\left(UV^2+f\xi\right)$$

We take,

$$\frac{d}{d\xi}(JIF) = -IF\,Pr(\gamma - 1)M^2{}_o\left(UV^2 + f\xi\right)$$

or

$$\int_0^{\xi} d(JIF) = -\int_0^{\xi} IF\,Pr(\gamma - 1)M^2{}_o\left(UV^2 + f\xi\right)d\xi$$

$$J(\xi) - J(\xi = 0) = -\frac{1}{IF}\int_0^{\xi} IF\,Pr(\gamma - 1)M^2{}_o\left(UV^2 + f\xi\right)d\xi$$

$$\xi\frac{d\Theta}{d\xi} - \left[\xi\frac{d\Theta}{d\xi}\right]_{\xi=0} = -\frac{1}{IF}\int_0^{\xi} IF\,Pr(\gamma - 1)M^2{}_o\left(UV^2 + f\xi\right)d\xi$$

Since

$$\left[\xi\frac{d\Theta}{d\xi}\right]_{\xi=0} = 0$$

$$\frac{d\Theta}{d\xi} = -\frac{1}{IF\xi}\int_0^{r} IF\,Pr(\gamma - 1)M^2{}_o\left(UV^2 + f\xi\right)d\xi$$

$$\frac{d\Theta}{d\xi} = -\Pr(\gamma-1)M^2{}_o\left[\frac{\left(1+\beta_2\xi^2\right)^{\frac{Pr\kappa}{2\beta_2}}}{\left(1+\beta_1\xi^2\right)^{\frac{Pr}{2\beta_1}}}\right]^{\lambda}\frac{1}{\xi}\int_0^{\xi}\left[\frac{\left(1+\beta_1\xi^2\right)^{\frac{Pr}{2\beta_1}}}{\left(1+\beta_2\xi^2\right)^{\frac{Pr\kappa}{2\beta_2}}}\right]^{\lambda}\left(UV^2+f\xi\right)d\xi$$

Separation of variables yields,

$$d\Theta = -\Pr(\gamma-1)M^2{}_o\left\{\left[\frac{\left(1+\beta_2\xi^2\right)^{\frac{Pr\kappa}{2\beta_2}}}{\left(1+\beta_1\xi^2\right)^{\frac{Pr}{2\beta_1}}}\right]^{\lambda}\frac{1}{\xi}\int_0^{\xi}\left[\frac{\left(1+\beta_1\xi^2\right)^{\frac{Pr}{2\beta_1}}}{\left(1+\beta_2\xi^2\right)^{\frac{Pr\kappa}{2\beta_2}}}\right]^{\lambda}\left(UV^2+f\xi\right)d\xi\right\}d\xi$$

Integration of both sides gives

$$\Theta-\Theta(\xi=0) = -\Pr(\gamma-1)M^2{}_o\int_0^{\xi}\left\{\left[\frac{\left(1+\beta_2\xi^2\right)^{\frac{Pr\kappa}{2\beta_2}}}{\left(1+\beta_1\xi^2\right)^{\frac{Pr}{2\beta_1}}}\right]^{\lambda}\frac{1}{\xi}\int_0^{\xi}\left[\frac{\left(1+\beta_1\xi^2\right)^{\frac{Pr}{2\beta_1}}}{\left(1+\beta_2\xi^2\right)^{\frac{Pr\kappa}{2\beta_2}}}\right]^{\lambda}\left(UV^2+f\xi\right)d\xi\right\}d\xi$$

or

$$\Theta = -\Pr(\gamma-1)M^2{}_o\int_0^{\xi}\left\{\left[\frac{\left(1+\beta_2\xi^2\right)^{\frac{Pr\kappa}{2\beta_2}}}{\left(1+\beta_1\xi^2\right)^{\frac{Pr}{2\beta_1}}}\right]^{\lambda}\frac{1}{\xi}\int_0^{\xi}\left[\frac{\left(1+\beta_1\xi^2\right)^{\frac{Pr}{2\beta_1}}}{\left(1+\beta_2\xi^2\right)^{\frac{Pr\kappa}{2\beta_2}}}\right]^{\lambda}\left(UV^2+f\xi\right)d\xi\right\}d\xi+\Theta_o$$

where $\Theta_o=\Theta(\xi=0)$

We do not know what the temperature is at $\xi = 0$, but we do know that, as $\xi \to \infty$,

$\Theta_\infty \to 1$(remember that $\Theta = T / T_\infty$)

$$1 = -Pr(\gamma - 1)M^2{}_o \int_0^\infty \left\{ \left[\frac{\left(1 + \beta_2 \xi^2\right)^{\frac{Pr\,\kappa}{2\beta_2}}}{\left(1 + \beta_1 \xi^2\right)^{\frac{Pr}{2\beta_1}}} \right]^\lambda \frac{1}{\xi} \int_0^\xi \left[\frac{\left(1 + \beta_1 \xi^2\right)^{\frac{Pr}{2\beta_1}}}{\left(1 + \beta_2 \xi^2\right)^{\frac{Pr\,\kappa}{2\beta_2}}} \right]^\lambda \left(UV^2 + f\xi\right) d\xi \right\} d\xi + \Theta_o$$

or

$$\Theta_o = Pr(\gamma - 1)M^2{}_o \int_0^\infty \left\{ \left[\frac{\left(1 + \beta_2 \xi^2\right)^{\frac{Pr\,\kappa}{2\beta_2}}}{\left(1 + \beta_1 \xi^2\right)^{\frac{Pr}{2\beta_1}}} \right]^\lambda \frac{1}{\xi} \int_0^\xi \left[\frac{\left(1 + \beta_1 \xi^2\right)^{\frac{Pr}{2\beta_1}}}{\left(1 + \beta_2 \xi^2\right)^{\frac{Pr\,\kappa}{2\beta_2}}} \right]^\lambda \left(UV^2 + f\xi\right) d\xi \right\} d\xi + 1 \tag{27}$$

Then

$$\Theta = -\Pr(\gamma - 1)M^2{}_o \int_0^\xi \left\{ \left[\frac{\left(1 + \beta_2 \xi^2\right)^{\frac{\Pr\,\kappa}{2\beta_2}}}{\left(1 + \beta_1 \xi^2\right)^{\frac{\Pr}{2\beta_1}}} \right]^\lambda \frac{1}{\xi} \int_0^\xi \left[\frac{\left(1 + \beta_1 \xi^2\right)^{\frac{\Pr}{2\beta_1}}}{\left(1 + \beta_2 \xi^2\right)^{\frac{\Pr\,\kappa}{2\beta_2}}} \right]^\lambda \left(UV^2 + f\xi\right) d\xi \right\} d\xi +$$

$$+Pr(\gamma - 1)M^2{}_o \int_0^\infty \left\{ \left[\frac{\left(1 + \beta_2 \xi^2\right)^{\frac{Pr\,\kappa}{2\beta_2}}}{\left(1 + \beta_1 \xi^2\right)^{\frac{Pr}{2\beta_1}}} \right]^\lambda \frac{1}{\xi} \int_0^\xi \left[\frac{\left(1 + \beta_1 \xi^2\right)^{\frac{Pr}{2\beta_1}}}{\left(1 + \beta_2 \xi^2\right)^{\frac{Pr\,\kappa}{2\beta_2}}} \right]^\lambda \left(UV^2 + f\xi\right) d\xi \right\} d\xi + 1$$

For the computations we have to use dummy variables, say t and s.

Then

$$\frac{d\Theta}{d\xi} = -Pr(\gamma-1)M^2{}_o \frac{\left(1+\beta_2\xi^2\right)^{\frac{Pr\kappa}{2\beta_2}}}{\left(1+\beta_1\xi^2\right)^{\frac{Pr}{2\beta_1}}\xi}\int_0^{\xi}\frac{\left(1+\beta_1 t^2\right)^{\frac{Pr}{2\beta_1}}}{\left(1+\beta_2 t^2\right)^{\frac{Pr\kappa}{2\beta_2}}}\left(U(t)V(t)^2+tf(t)\right)dt$$

and

$$\Theta = -Pr(\gamma-1)M^2{}_o\int_0^{\xi}\left\{\frac{\left(1+\beta_2 s^2\right)^{\frac{Pr\kappa}{2\beta_2}}}{\left(1+\beta_1 s^2\right)^{\frac{Pr}{2\beta_1}}s}\int_0^{s}\frac{\left(1+\beta_1 t^2\right)^{\frac{Pr}{2\beta_1}}}{\left(1+\beta_2 t^2\right)^{\frac{Pr\kappa}{2\beta_2}}}\left(U(t)V(t)^2+tf(t)\right)dt\right\}ds$$

$$+Pr(\gamma-1)M^2{}_o\int_0^{\infty}\left\{\frac{\left(1+\beta_2 s^2\right)^{\frac{Pr\kappa}{2\beta_2}}}{\left(1+\beta_1 s^2\right)^{\frac{Pr}{2\beta_1}}s}\int_0^{s}\frac{\left(1+\beta_1 t^2\right)^{\frac{Pr}{2\beta_1}}}{\left(1+\beta_2 t^2\right)^{\frac{Pr\kappa}{2\beta_2}}}\left(U(t)V(t)^2+tf(t)\right)dt\right\}ds+1$$

For this project case, the relation used for U,V,λ and f are given below:

$$U\frac{1}{\xi}\frac{d}{d\xi}(\xi V) = \frac{d}{d\xi}\left(\frac{1}{\xi}\frac{d}{d\xi}(\xi V)\right)$$

$$U = -\lambda\left[\frac{\xi}{1+\beta_1\xi^2} - \frac{\kappa\xi}{1+\beta_2\xi^2}\right]$$

$$V=\frac{1}{\xi}\frac{\int_0^{\xi}\left[\frac{\left(1+\beta_2\xi^2\right)^{\frac{\kappa}{2\beta_2}}}{\left(1+\beta_1\xi^2\right)^{\frac{1}{2\beta_1}}}\right]^{\lambda}\xi d\xi}{\int_0^{1}\left[\frac{\left(1+\beta_2\xi^2\right)^{\frac{\kappa}{2\beta_2}}}{\left(1+\beta_1\xi^2\right)^{\frac{1}{2\beta_1}}}\right]^{\lambda}\xi d\xi}$$

The value of λ is obtained by the equation below:

$$\left[\frac{\left(1+\beta_1\right)^{\frac{1}{2\beta_1}}}{\left(1+\beta_2\right)^{\frac{\kappa}{2\beta_2}}}\right]^{\lambda}-\int_0^{1}\left[\frac{\left(1+\beta_1\xi^2\right)^{\frac{1}{2\beta_1}}}{\left(1+\beta_2\xi^2\right)^{\frac{\kappa}{2\beta_2}}}\right]^{\lambda}\xi d\xi=0$$

$$f=\left[\xi\frac{d}{d\xi}\left(\frac{V}{\xi}\right)\right]^2=\left[\frac{\left\{\frac{\left(1+\beta_2\xi^2\right)^{\frac{\kappa}{2\beta_2}}}{\left(1+\beta_1\xi^2\right)^{\frac{1}{2\beta_1}}}\right\}^{\lambda}-\frac{2}{\xi^2}\int_0^{\xi}\left\{\frac{\left(1+\beta_2\xi^2\right)^{\frac{\kappa}{2\beta_2}}}{\left(1+\beta_1\xi^2\right)^{\frac{1}{2\beta_1}}}\right\}^{\lambda}\xi d\xi}{\int_0^{1}\left\{\frac{\left(1+\beta_2\xi^2\right)^{\frac{\kappa}{2\beta_2}}}{\left(1+\beta_1\xi^2\right)^{\frac{1}{2\beta_1}}}\right\}^{\lambda}\xi d\xi}\right]^2$$

2. Transformation of Steady Vortices into time decay

❒ Transformation of Navier-Stokes equations into time dependent:

- **Tangential momentum**

From dimensional analysis we know that:

$$V_\theta = \frac{\kappa}{r} f\left(\frac{r^2}{\nu t}\right)$$

Or

$$V_\theta = \frac{\kappa}{r} f\left(\frac{r^2}{4\nu t}\right) \quad \rightarrow \quad V_\theta = \frac{\kappa}{R r_c} f\left(\frac{\xi^2}{\chi}\right)$$

From dimensionalization we know that $\xi = r / r_c$

and $\chi = 1 + \tau$, $\left(\tau = \frac{\nu t}{r^2{}_c}\right)$

Therefore, the tangential velocity distribution is given by

$$V(\chi, \xi) = \frac{V_\theta r_C}{\kappa} = \frac{1}{\xi} f\left(\frac{\xi^2}{\chi}\right)$$

From Eq. (2.2.3.a)

$$\xi = \eta\sqrt{1+\tau}$$

Hence, variable η contains both radius (ξ) and time (τ).

Then, the tangential velocity transforms into,

$$V(\tau,\xi)=\frac{1}{\eta\sqrt{1+\tau}}f(\eta^2)\rightarrow V(\eta)=V(\tau,\xi)\sqrt{1+\tau}=\frac{1}{\eta}f(\eta^2),$$

Where $V(\eta)=\frac{1}{\eta}f(\eta^2)$

The tangential velocity is further converted to:

$$V(\tau,\xi)=\frac{g(\eta)}{\sqrt{1+\tau}}\rightarrow V(\eta)=V(\tau,\xi)\sqrt{1+\tau}=\frac{1}{\eta}f(\eta^2)=g(\eta)$$

Based on order of magnitude arguments, the obtained tangential momentum is:

Tangential-momentum:

$$\frac{\partial V}{\partial\tau}+Re\cdot u(\tau,\xi)\left(\frac{\partial V}{\partial\xi}+\frac{V}{\xi}\right)=\frac{\partial^2 V}{\partial\xi^2}+\frac{1}{\xi}\frac{\partial V}{\partial\xi}-\frac{V}{\xi^2}$$

(i) (ii) (iii) (iv) (v)

Separating the tangential momentum in parts, we obtain:

Part (i)

Taking the derivative of tangential velocity with respect to time, we take:

$$\frac{\partial V}{\partial\tau}=\frac{\partial}{\partial\tau}\left(\frac{g}{\sqrt{1+\tau}}\right)=-\frac{1}{2(1+\tau)^{3/2}}g+\frac{1}{\sqrt{1+\tau}}g'\frac{\partial\eta}{\partial\tau}$$

Where $g'\equiv\frac{dg}{\partial\eta}$

and $\frac{\partial \eta}{\partial \tau} = -\frac{1}{2}\frac{\xi}{(1+\tau)^{3/2}}$

$$\frac{\partial V}{\partial \tau} = \frac{\partial}{\partial \tau}\left(\frac{g}{\sqrt{1+\tau}}\right) = -\frac{1}{2(1+\tau)^{3/2}} g - \frac{1}{2}\frac{1}{(1+\tau)^{3/2}}\frac{\xi}{\sqrt{1+\tau}} g' = -\frac{1}{2(1+\tau)^{3/2}}\left(g + \frac{\xi}{\sqrt{1+\tau}} g'\right)$$

Therefore, part (i) becomes,

$$\frac{\partial V}{\partial \tau} = -\frac{1}{2(1+\tau)^{3/2}}(g + \eta g') = -\frac{1}{2(1+\tau)^{3/2}}\frac{d}{d\eta}(\eta g)$$

Part (iv)

Taking the derivative of tangential velocity with respect to radius, we take:

$$\frac{\partial V}{\partial \xi} = \frac{\partial}{\partial \eta}\left(\frac{g}{\sqrt{1+\tau}}\right)\frac{\partial \eta}{\partial \xi} = \frac{1}{\sqrt{1+\tau}} g' \frac{\partial \eta}{\partial \xi} = \frac{1}{1+\tau} g' \frac{\partial \eta}{\partial \xi}$$

$$\frac{\partial V}{\partial \xi} = \frac{\partial}{\partial \eta}\left(\frac{g}{\sqrt{1+\tau}}\right)\frac{\partial \eta}{\partial \xi} = \frac{1}{\sqrt{1+\tau}} g' \frac{\partial \eta}{\partial \xi} = \frac{1}{1+\tau} g' \quad , \qquad (a)$$

where the derivative of η with respect to radius is:

$$\frac{\partial \eta}{\partial \xi} = \frac{1}{\sqrt{1+\tau}}$$

Multiplying by ξ the above equation becomes,

$$\frac{1}{\xi}\frac{\partial V}{\partial \xi} = \frac{\partial}{\partial \eta}\left(\frac{g}{\sqrt{1+\tau}}\right)\frac{\partial \eta}{\partial \xi} = \frac{1}{\sqrt{1+\tau}} g' \frac{\partial \eta}{\partial \xi} = \frac{1}{(1+\tau)\xi} g'$$

Therefore, part (iv) yields,

$$\frac{1}{\xi}\frac{\partial V}{\partial \xi}=\frac{\partial}{\partial \eta}\left(\frac{g}{\sqrt{1+\tau}}\right)\frac{\partial \eta}{\partial \xi}=\frac{1}{\sqrt{1+\tau}}g'\frac{\partial \eta}{\partial \xi}=\frac{1}{(1+\tau)\xi}g'$$

Part (iii)

Differentiating the Eq. (a) at part (iv) once more gives:

$$\frac{\partial^2 V}{\partial \xi^2}=\frac{\partial}{\partial \xi}\left(\frac{\partial V}{\partial \xi}\right)=\frac{\partial}{\partial \eta}\left(\frac{1}{1+\tau}g'\right)\frac{\partial \eta}{\partial \xi}=\frac{1}{(1+\tau)^{3/2}}g''$$

Therefore, part (iii) becomes,

$$\frac{\partial^2 V}{\partial \xi^2}=\frac{\partial}{\partial \xi}\frac{\partial v}{\partial \xi}=\frac{\partial}{\partial \eta}\left(\frac{1}{1+\tau}g'\right)\frac{\partial \eta}{\partial \xi}=\frac{1}{(1+\tau)^{3/2}}g''$$

Part (v)

We know from Eq. (2.2.2), that

$$V(\eta)=V(\tau,\xi)\sqrt{1+\tau}\rightarrow V(\tau,\xi)=\frac{V(\eta)}{\sqrt{1+\tau}}=\frac{g}{\sqrt{1+\tau}}$$

Therefore, the term (v) becomes,

$$\frac{V(\tau,\xi)}{\xi^2}=\frac{g}{\sqrt{1+\tau}\xi^2}$$

Part (ii)

We know that,

$$\frac{V(\tau,\xi)}{\xi}=\frac{g}{\sqrt{1+\tau}\xi}$$

Taking the derivative of the above equation, we obtain

$$\frac{\partial V}{\partial \xi}=\frac{1}{1+\tau}g'$$

$$u(\tau,\xi)\left(\frac{\partial V}{\partial \xi}+\frac{V}{\xi}\right)=u(\tau,\xi)\left(\frac{1}{1+\tau}g'+\frac{g}{\sqrt{1+\tau}\xi}\right)$$

Therefore, the term (iv) becomes,

$$u(\tau,\xi)\left(\frac{\partial V}{\partial \xi}+\frac{V}{\xi}\right)=u(\tau,\xi)\left(\frac{1}{1+\tau}g'+\frac{g}{\sqrt{1+\tau}\xi}\right)$$

Inserting the parts (i), (ii), (iii), (iv) and (v) in the tangential momentum yields:

$$-\frac{1}{2(1+\tau)^{3/2}}\frac{d}{d\eta}(\eta g)+Reu(\tau,\xi)\left(\frac{1}{1+\tau}g'+\frac{g}{\sqrt{1+\tau}\xi}\right)=\frac{1}{(1+\tau)^{3/2}}g''+\frac{1}{(1+\tau)\xi}g'-\frac{g}{\sqrt{1+\tau}\xi^2}\rightarrow$$

$$-\frac{1}{2(1+\tau)^{3/2}}\frac{d}{d\eta}(\eta g)+Reu(\tau,\xi)\left(\frac{1}{1+\tau}g'+\frac{g}{\sqrt{1+\tau}\xi}\right)=\frac{1}{(1+\tau)^{3/2}}\left[g''+\frac{\sqrt{1+\tau}}{\xi}g'-\frac{1+\tau}{\xi^2}g\right]\rightarrow$$

$$-\frac{1}{2(1+\tau)^{3/2}}\frac{d}{d\eta}(\eta g)+Reu(\tau,\xi)\left(\frac{1}{1+\tau}g'+\frac{g}{(1+\tau)\eta}\right)=\frac{1}{(1+\tau)^{3/2}}\left[g''+\frac{1}{\frac{\xi}{\sqrt{1+\tau}}}g'-\frac{g}{\frac{\xi^2}{1+\tau}}\right]\rightarrow$$

$$-\frac{1}{2(1+\tau)^{3/2}}\frac{d}{d\eta}(\eta g)+\frac{Reu(\tau,\xi)}{1+\tau}\left(g'+\frac{g}{\eta}\right)=\frac{1}{(1+\tau)^{3/2}}\left[g''+\frac{1}{\frac{\xi}{\sqrt{1+\tau}}}g'-\frac{g}{\frac{\xi^2}{1+\tau}}\right]\rightarrow$$

$$-\frac{\eta}{2}\frac{1}{\eta}\frac{d}{d\eta}(\eta g)+Reu(\tau,\xi)\sqrt{1+\tau}\frac{1}{\eta}\frac{d}{d\eta}(g\eta)=g''+\frac{1}{\eta}g'-\frac{g}{\eta^2}\rightarrow$$

$$\left\{Reu(\tau,\xi)\sqrt{1+\tau}-\frac{\eta}{2}\right\}\frac{1}{\eta}\frac{d}{d\eta}(g\eta)=g''+\frac{1}{\eta}g'-\frac{g}{\eta^2}$$

$$\left\{Reu(\tau,\xi)\sqrt{1+\tau}-\frac{\eta}{2}\right\}\frac{1}{\eta}\frac{d}{d\eta}(g\eta)=g''+\frac{1}{\eta}g'-\frac{g}{\eta^2}$$

The analytical mathematical process is produced in Appendix A.

If we take $U(\eta)=Reu(\tau,\xi)\sqrt{1+\tau}-\frac{\eta}{2}$

then we obtain:

$$\frac{U(\eta)}{\eta}\frac{d}{d\eta}(g\eta)=g''+\frac{1}{\eta}g'-\frac{g}{\eta^2}$$

The previous equation is the same as the steady state where we know several solutions.

- **Conservation of mass:**

$$\frac{\partial u}{\partial \xi} + \frac{u}{\xi} + h = 0$$

(i) (ii) (iii)

Where, $\eta = \dfrac{\xi}{\sqrt{1+\tau}}$

Based on transformation relations, we take:

$$U(\eta) = u(\tau,\xi) Re\sqrt{1+\tau} - \frac{\eta}{2} \rightarrow u(\tau,\xi) = \frac{1}{Re}\left(\frac{U(\eta)}{\sqrt{1+\tau}} + \frac{\eta}{2\sqrt{1+\tau}}\right)$$

Separating the conservation of mass in parts and we obtain:

Part (i)

$$\frac{\partial u}{\partial \xi} = \frac{\partial}{\partial \eta}\left[\frac{1}{Re}\left(\frac{U(\eta)}{\sqrt{1+\tau}} + \frac{\eta}{2\sqrt{1+\tau}}\right)\right]\frac{\partial \eta}{\partial \xi}, \quad \text{where } \frac{\partial \eta}{\partial \xi} = \frac{1}{\sqrt{1+\tau}}$$

$$\frac{\partial u}{\partial \xi} = \frac{\partial}{\partial \eta}\left[\frac{1}{Re}\left(\frac{U(\eta)}{\sqrt{1+\tau}} + \frac{\eta}{2\sqrt{1+\tau}}\right)\right]\frac{1}{\sqrt{1+\tau}} \rightarrow \frac{\partial u}{\partial \xi} = \frac{1}{Re}\left(\frac{1}{1+\tau}\frac{\partial U(\eta)}{\partial \eta} + \frac{1}{2(1+\tau)}\right)$$

Therefore, term (i) becomes

$$\frac{\partial u}{\partial \xi} = \frac{1}{Re}\left(\frac{1}{1+\tau}\frac{\partial U(\eta)}{\partial \eta} + \frac{1}{2(1+\tau)}\right)$$

Part (ii)

$$\frac{u}{\xi} = \frac{1}{\xi}\left[\frac{1}{Re}\left(\frac{U(\eta)}{\sqrt{1+\tau}} + \frac{\eta}{2\sqrt{1+\tau}}\right)\right], \text{ where } \xi = \eta\sqrt{1+\tau}$$

$$\rightarrow \frac{u}{\xi} = \frac{1}{\eta\sqrt{1+\tau}}\left[\frac{1}{Re}\left(\frac{U(\eta)}{\sqrt{1+\tau}} + \frac{\eta}{2\sqrt{1+\tau}}\right)\right] \rightarrow \frac{u}{\xi} = \frac{1}{Re}\left(\frac{U(\eta)}{\eta(1+\tau)} + \frac{1}{2(1+\tau)}\right)$$

Therefore, part (ii) becomes:

$$\frac{u}{\xi} = \frac{1}{Re}\left(\frac{U(\eta)}{\eta(1+\tau)} + \frac{1}{2(1+\tau)}\right)$$

Part (iii)

From the transformation relations, we take the axial velocity:

$$H(\eta) = 1 + h(\tau,\xi)\,Re(1+\tau) \rightarrow h(\tau,\xi) = \frac{1}{Re}\left(\frac{H(\eta)}{1+\tau} - \frac{1}{1+\tau}\right)$$

Therefore, part (iii) yields:

$$h(\tau,\xi) = \frac{1}{Re}\left(\frac{H(\eta)}{1+\tau} - \frac{1}{1+\tau}\right)$$

Inserting the parts (i), (ii) and (iii) into conservation of mass we have:

$$\frac{1}{Re}\left(\frac{1}{1+\tau}\frac{\partial U(\eta)}{\partial \eta} + \frac{1}{2(1+\tau)}\right) + \frac{1}{Re}\left(\frac{U(\eta)}{\eta(1+\tau)} + \frac{1}{2(1+\tau)}\right) + \frac{1}{Re}\left(\frac{H(\eta)}{1+\tau} - \frac{1}{1+\tau}\right) = 0$$

$$\rightarrow \frac{\partial U}{\partial \eta} + \frac{U}{\eta} + H(\eta) = 0$$

- **Radial-momentum**

$$\frac{V^2}{\xi} = \frac{\partial P}{\partial \xi}$$

(i) (ii)

Based on transformation relations, we take:

$$\bar{V}(\eta) = V(\tau,\xi)\sqrt{1+\tau} \Rightarrow V(\tau,\xi) = \frac{V(\eta)}{\sqrt{1+\tau}}$$

Divided the radial momentum in terms and we obtain:

Part (i)

$$\frac{V^2}{\xi} = \frac{\left(\frac{V(\eta)}{\sqrt{1+\tau}}\right)^2}{\eta\sqrt{1+\tau}} = \frac{V^2(\eta)}{\eta(1+\tau)\sqrt{1+\tau}}, \quad \text{where } \xi = \eta\sqrt{1+\tau}$$

Therefore, part (i) yields:

$$\frac{V^2}{\xi} = \frac{V^2(\eta)}{\eta(1+\tau)\sqrt{1+\tau}}$$

Part (ii)

From the transformation relations, we take the pressure distribution:

$$\Delta\Pi = (1+\tau)p(\tau,\xi) \rightarrow p(\tau,\xi) = \frac{\Delta\Pi}{(1+\tau)}$$

Where $\frac{\partial\eta}{\partial\xi} = \frac{1}{\sqrt{1+\tau}}$

$$\frac{\partial p}{\partial\xi} = \frac{\partial}{\partial\eta}\left(\frac{\Delta\Pi}{(1+\tau)}\right)\frac{\partial\eta}{\partial\xi} \rightarrow \frac{\partial p}{\partial\xi} = \frac{\partial}{\partial\eta}\left(\frac{\Delta\Pi}{(1+\tau)}\right)\frac{1}{\sqrt{1+\tau}} \rightarrow \frac{\partial p}{\partial\xi} = \frac{1}{(1+\tau)\sqrt{1+\tau}}\frac{\partial\Delta\Pi}{\partial\eta}$$

Therefore, part (ii) becomes:

$$\frac{\partial p}{\partial\xi} = \frac{1}{(1+\tau)\sqrt{1+\tau}}\frac{\partial\Delta\Pi}{\partial\eta}$$

From radial momentum, we take

$$\frac{V^2(\eta)}{\eta(1+\tau)\sqrt{1+\tau}} = \frac{1}{(1+\tau)\sqrt{1+\tau}}\frac{\partial \Delta\Pi}{\partial \eta} \rightarrow \frac{V^2(\eta)}{\eta} = \frac{\partial \Delta\Pi}{\partial \eta}$$

The radial momentum becomes:

$$\frac{V^2(\eta)}{\eta} = \frac{\partial \Delta\Pi}{\partial \eta}$$

❒ **Transformation of the two cell steady vortices into time decay:**

For our case the two cell steady solution:

$$V=\frac{1}{\xi}\frac{\int_0^{\xi}\left[\frac{\left(1+\beta_2\xi^2\right)^{\frac{\kappa}{2\beta_2}}}{\left(1+\beta_1\xi^2\right)^{\frac{1}{2\beta_1}}}\right]^{\lambda}\xi d\xi}{Y_{\infty}}$$

is known. To transform this into decaying vortex we replace on the right hand side R by $\eta=\frac{\xi}{\sqrt{1+\tau}}$.

$$V=\frac{1}{\eta}\frac{\int_0^{\eta}\left[\frac{\left(1+\beta_2\eta^2\right)^{\frac{\kappa}{2\beta_2}}}{\left(1+\beta_1\eta^2\right)^{\frac{1}{2\beta_1}}}\right]^{\lambda}\eta d\eta}{\int_0^{1}\left[\frac{\left(1+\beta_2\eta^2\right)^{\frac{\kappa}{2\beta_2}}}{\left(1+\beta_1\eta^2\right)^{\frac{1}{2\beta_1}}}\right]^{\lambda}\eta d\eta}$$

On the left hand side we have

$$\bar{V}(\eta)=V(\tau,\xi)\sqrt{1+\tau}$$

Then,

$$V(\tau,\xi)\sqrt{1+\tau}=\frac{1}{\frac{\xi}{\sqrt{1+\tau}}}\frac{\int_0^{\eta}\left[\frac{\left(1+\beta_2\eta^2\right)^{\frac{\kappa}{2\beta_2}}}{\left(1+\beta_1\eta^2\right)^{\frac{1}{2\beta_1}}}\right]^{\lambda}\eta d\eta}{Y(\infty)}$$

or

$$V(\tau,\xi)=\frac{1}{\frac{\xi}{\sqrt{1+\tau}}\sqrt{1+\tau}}\frac{\int_0^{\frac{\xi}{\sqrt{1+\tau}}}\left[\frac{\left(1+\beta_2\left[\frac{\xi}{\sqrt{1+\tau}}\right]^2\right)^{\frac{\kappa}{2\beta_2}}}{\left(1+\beta_1\left[\frac{\xi}{\sqrt{1+\tau}}\right]^2\right)^{\frac{1}{2\beta_1}}}\right]^{\lambda}\frac{\xi}{\sqrt{1+\tau}}d\frac{\xi}{\sqrt{1+\tau}}}{Y(\infty)}$$

$$V(\tau,\xi)=\frac{1}{\xi(1+\tau)}\frac{\int_0^{\frac{\xi}{\sqrt{1+\tau}}}\left[\frac{\left(1+\beta_2\left[\frac{\xi}{\sqrt{1+\tau}}\right]^2\right)^{\frac{\kappa}{2\beta_2}}}{\left(1+\beta_1\left[\frac{\xi}{\sqrt{1+\tau}}\right]^2\right)^{\frac{1}{2\beta_1}}}\right]^{\lambda}\xi d\xi}{Y(\infty)}$$

- **Axial velocity:**

$$h=2\lambda\left[\frac{1}{\left(1+\beta_1\xi^2\right)^2}-\frac{\kappa}{\left(1+\beta_2\xi^2\right)^2}\right]$$

is known. To transform this into decaying vortex we replace on the right hand side radius by

$$\eta=\frac{\xi}{\sqrt{1+\tau}}.$$

$$H(\eta)=2\lambda\left[\frac{1}{\left(1+\beta_1\eta^2\right)^2}-\frac{\kappa}{\left(1+\beta_2\eta^2\right)^2}\right]$$

On the left hand side we have

$$H(\eta) = 1 + h(\tau,\xi)\,Re(1+\tau)$$

Then,

$$1 + h(\tau,\xi)\,Re(1+\tau) = 2\lambda\left[\frac{1}{(1+\beta_1\eta^2)^2} - \frac{\kappa}{(1+\beta_2\eta^2)^2}\right] \rightarrow$$

$$h(\tau,\xi)\,Re = \frac{1}{(1+\tau)}\left[\left(\frac{1}{\left(1+\beta_1\frac{\xi^2}{1+\tau}\right)^2} - \frac{\kappa}{\left(1+\beta_2\frac{\xi^2}{1+\tau}\right)^2}\right)2\lambda - 1\right]$$

- **Radial Velocity:**

$$u = -\lambda\left[\frac{\xi}{1+\beta_1\xi^2} - \frac{\kappa\xi}{1+\beta_2\xi^2}\right]$$

is known. To transform this into decaying vortex we replace on the right hand side radius by

$$\eta = \frac{\xi}{\sqrt{1+\tau}}.$$

$$U(\eta) = -\lambda\left[\frac{\eta}{1+\beta_1\eta^2} - \frac{\kappa\eta}{1+\beta_2\eta^2}\right]$$

On the left side we have,

$$U(\eta) = u(\tau,\xi) Re\sqrt{1+\tau} - \frac{\eta}{2}$$

Then,

$$u(\tau,\xi) Re\sqrt{1+\tau} - \frac{\eta}{2} = -\lambda\left[\frac{\eta}{1+\beta_1\eta^2} - \frac{\kappa\eta}{1+\beta_2\eta^2}\right] \rightarrow$$

$$u(\tau,\xi) Re\sqrt{1+\tau} - \frac{\frac{\xi}{\sqrt{1+\tau}}}{2} = -\lambda\left[\frac{\frac{\xi}{\sqrt{1+\tau}}}{1+\beta_1\left(\frac{\xi}{\sqrt{1+\tau}}\right)^2} - \frac{\kappa\frac{\xi}{\sqrt{1+\tau}}}{1+\beta_2\left(\frac{\xi}{\sqrt{1+\tau}}\right)^2}\right] \rightarrow$$

$$u(\tau,\xi) Re = \frac{\xi}{1+\tau}\left[\frac{1}{2} - \left(\frac{1}{1+\beta_1\frac{\xi^2}{1+\tau}} - \frac{\kappa}{1+\beta_2\frac{\xi^2}{1+\tau}}\right)\lambda\right]$$

Appendix B

- **The source code for solving the equations in MATLAB**

```
clear all
close all
clc
format long
gamma=1.4;
r=10;
n=1000;
h =(r)/n;
M0=0.6;
Pr=2/3;
k1=1;
k2=1.10;
b1=0.375;
b2=0.6;
lambda=222.3064314012514;
Y_oo1= 4.371312757954488; % limit r=10
Y_oo2= 3.996199251028413; % limit r=1===Integral_22
Integral_22= integral (@(x)((((1+(b1*(x.^2))).^((-
k1)./(2*b1))).*((1+(b2*(x.^2))).^(k2./(2*b2)))).^lambda).*x,0,1);




sum5=zeros(1,1);
sum6=zeros(1,1);

for A=1:1:n
   d=A*h;
   o=(d-h/2);
   z=o;

F1= @(x) ((((1+(b1*(x.^2))).^((-
k1)./(2*b1))).*((1+(b2*(x.^2))).^(k2./(2*b2)))).^lambda).*x;
```

```
Upper_Integral= quadl(F1,0,o);
V= Upper_Integral./(o.*Integral_22);
F2= @(x) ((-lambda).*(((k1*x)./(1+(b1*(x.^2))))-((k2*x)./(1+(b2*(x.^2))))));
U=F2(o);
F3= @(x)((((1+(b1*(x.^2))).^((-
k1)./(2*b1))).*((1+(b2*(x.^2))).^(k2./(2*b2)))).^lambda);
F4= @(x) ((((1+(b1*(x.^2))).^((-
k1)./(2*b1))).*((1+(b2*(x.^2))).^(k2./(2*b2)))).^lambda).*x;
Upper_Integral2= quadl(F4,0,o);
F5= -((2./(o).^2).*Upper_Integral2);
F6=F3(o);
f=((1./Integral_22).*(F5+F6)).^2;
F70=@(x)
((((1+(b1*(x.^2))).^(((Pr)*k1)./(2*b1)))./((1+(b2*(x.^2))).^(((Pr)*k2)./(2*b2)))).^lam
bda);
F85(A)=F70(o);
height=@(o) F70(o).*((U.*(V.^2))+(o.*f));
sum5=sum5+(h*height(o));
M(A)=sum5;
F78=@(x)
((((1+(b2*(x.^2))).^(((Pr)*k2)./(2*b2)))./((1+(b1*(x.^2))).^(((Pr)*k1)./(2*b1)))).^lam
bda);
F73(A)=F78(z);
F74=@(x) (1./x);
F75(A)=F74(z);
d_Theta=@(z) (F73(A).*F75(A).*M(A));
sum6=sum6+(h*d_Theta(z));

end
theta_zero=(sum6.*((M0.^2).*(Pr).*(gamma-1)))+1;


sum=zeros(1,1);
sum2=zeros(1,1);
theta_z=zeros(n,1);
theta=zeros(n,1);
T1=zeros(n,1);
```

% theta (temperature)

```
for L=1:1:n
   j=L*h;
   i=(j-h/2);
   k=i;

F1= @(x) ((((1+(b1*(x.^2))).^((-
k1)./(2*b1))).*((1+(b2*(x.^2))).^(k2./(2*b2)))).^lambda).*x;
Upper_Integral= quadl(F1,0,i);
V= Upper_Integral./(i.*Integral_22);
F2= @(x) ((-lambda).*(((k1*x)./(1+(b1*(x.^2))))-((k2*x)./(1+(b2*(x.^2))))));
U=F2(i);
F3= @(x)((((1+(b1*(x.^2))).^((-
k1)./(2*b1))).*((1+(b2*(x.^2))).^(k2./(2*b2)))).^lambda);
F4= @(x) ((((1+(b1*(x.^2))).^((-
k1)./(2*b1))).*((1+(b2*(x.^2))).^(k2./(2*b2)))).^lambda).*x;
Upper_Integral2= quadl(F4,0,i);
F5= -((2./(i).^2).*Upper_Integral2);
F6=F3(i);
f=((1./Integral_22).*(F5+F6)).^2;
F70=@(x)
((((1+(b1*(x.^2))).^(((Pr)*k1)./(2*b1))))./((1+(b2*(x.^2))).^(((Pr)*k2)./(2*b2)))).^lam
bda);
F85(L)=F70(i);
height=@(i) F70(i).*((U.*(V.^2))+(i.*f));
sum=sum+(h*height(i));
Z(L)=sum;
F78=@(x)
((((1+(b2*(x.^2))).^(((Pr)*k2)./(2*b2))))./((1+(b1*(x.^2))).^(((Pr)*k1)./(2*b1)))).^lam
bda);
F73(L)=F78(k);
F74=@(x) (1./x);
F75(L)=F74(k);
d_Theta=@(k) (F73(L).*F75(L).*Z(L));
sum2=sum2+(h*d_Theta(k));
T1(L)=sum2.*((M0.^2).*(-Pr).*(gamma-1));
theta_z(L)= theta_zero;
theta(L)=theta_z(L)+T1(L);

end
plot(theta)
```

% pressure and density

```
for L=1:1:n
   j=L*h;
   i=(j-h/2);
   k=i;

F1= @(x) ((((1+(b1*(x.^2))).^((-
k1)./(2*b1))).*((1+(b2*(x.^2))).^(k2./(2*b2)))).^lambda).*x;
Upper_Integral= quadl(F1,0,i);
V= Upper_Integral./(i.*Integral_22);
F2= @(x) ((-lambda).*(((k1*x)./(1+(b1*(x.^2))))-((k2*x)./(1+(b2*(x.^2))))));
U=F2(i);
F3= @(x)((((1+(b1*(x.^2))).^((-
k1)./(2*b1))).*((1+(b2*(x.^2))).^(k2./(2*b2)))).^lambda);
F4= @(x) ((((1+(b1*(x.^2))).^((-
k1)./(2*b1))).*((1+(b2*(x.^2))).^(k2./(2*b2)))).^lambda).*x;
Upper_Integral2= quadl(F4,0,i);
F5= -((2./(i).^2).*Upper_Integral2);
F6=F3(i);
f=((1./Integral_22).*(F5+F6)).^2;
F70=@(x)
((((1+(b1*(x.^2))).^(((Pr)*k1)./(2*b1))))./((1+(b2*(x.^2))).^(((Pr)*k2)./(2*b2)))).^lam
bda);
F85(L)=F70(i);
height=@(i) F70(i).*((U.*(V.^2))+(i.*f));
sum=sum+(h*height(i));
Z(L)=sum;
F78=@(x)
((((1+(b2*(x.^2))).^(((Pr)*k2)./(2*b2))))./((1+(b1*(x.^2))).^(((Pr)*k1)./(2*b1)))).^lam
bda);
F73(L)=F78(k);
F74=@(x) (1./x);
F75(L)=F74(k);
d_Theta=@(k) (F73(L).*F75(L).*Z(L));
sum2=sum2+(h*d_Theta(k));
T1(L)=sum2.*((M0.^2).*(-Pr).*(gamma-1));
theta_z(L)= theta_zero;
theta(L)=theta_z(L)+T1(L);
```

```
Density=@(i) ((V.^2)./i);
sum9=sum9+(h*Density(i));
D1(L)=sum9;
D_zero(L)=Density_zero;
D_total(L)=D1(L)-D_zero(L);
Beta(L)= (1./(theta(L))).*(exp((gamma*(M0.^2)*D_total(L))./theta(L)));
Pressure(L)=Beta(L).*theta(L);
end



plot(Pressure)
```

❒ **Decaying vortices**

```
 clear all
close all
clc
format long
gamma=1.4;
r=10;
n=10000;
h =(r)/n; %h=0.001
M0=0.6;
Pr=2/3;
k1=1;
k2=1.10;
b1=0.375;
b2=0.6;
t=1;

lambda=222.3064314012514;
Y_oo1= 4.371312757954518;% limit r=10

Integral_22= integral (@(x)((((1+(b1*(x.^2))).^((-
k1)./(2*b1))).*((1+(b2*(x.^2))).^(k2./(2*b2)))).^lambda).*x,0,10);
```

% tangential velocity

```
for i=1:(n+1)
   x(i) = ((i-0.5)*h);
%x(i) = ((i-0.5)*h)./(t.^(1/2));%Integral is calculated at center of each node
end

for o=1:n
   F1= @(x) ((((1+(b1*((x./(t.^(1/2))).^2))).^((-
k1)./(2*b1))).*((1+(b2*((x./(t.^(1/2))).^2))).^(k2./(2*b2)))).^lambda).*x;
   Upper_Integral(o)= quadl(F1,0,x(o)./(t.^(1/2)));

   V(o)= Upper_Integral(o)./(x(o).*(Y_oo1).*t);

End
```

% radial and axial velocity

```
for i=1:(n+1)
x(i) = (i-0.5)*h ;%Integral is calculated at center of each node
end

for o=1:n
   F2= @(x)    (( x./t).*((1/2)-((lambda).*(((k1)./(1+(b1*((x.^2)./t))))-
((k2)./(1+(b2*((x.^2)./t)))))))));
   U(o)=F2(x(o));
   F3= @(x)    ((1./t).*(((2*lambda).*((k1./(1+(b1*((x.^2)./t))).^2)-
((k2)./(1+(b2*((x.^2)./t))).^2)))-1));
   H(o)=F3(x(o));
end
figure (1);
plot(U);
figure (2);
plot (H);
```